High precision measurement of the W boson mass at CDF

Chris Hays, Oxford University

La Thuile 2023
9 March

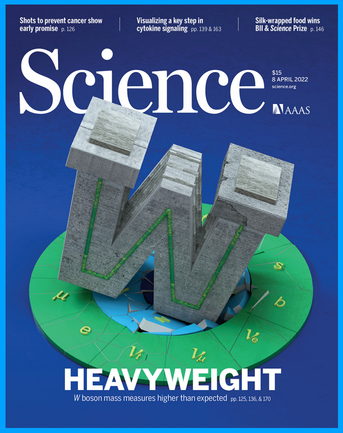

W boson mass

Higgs field potential

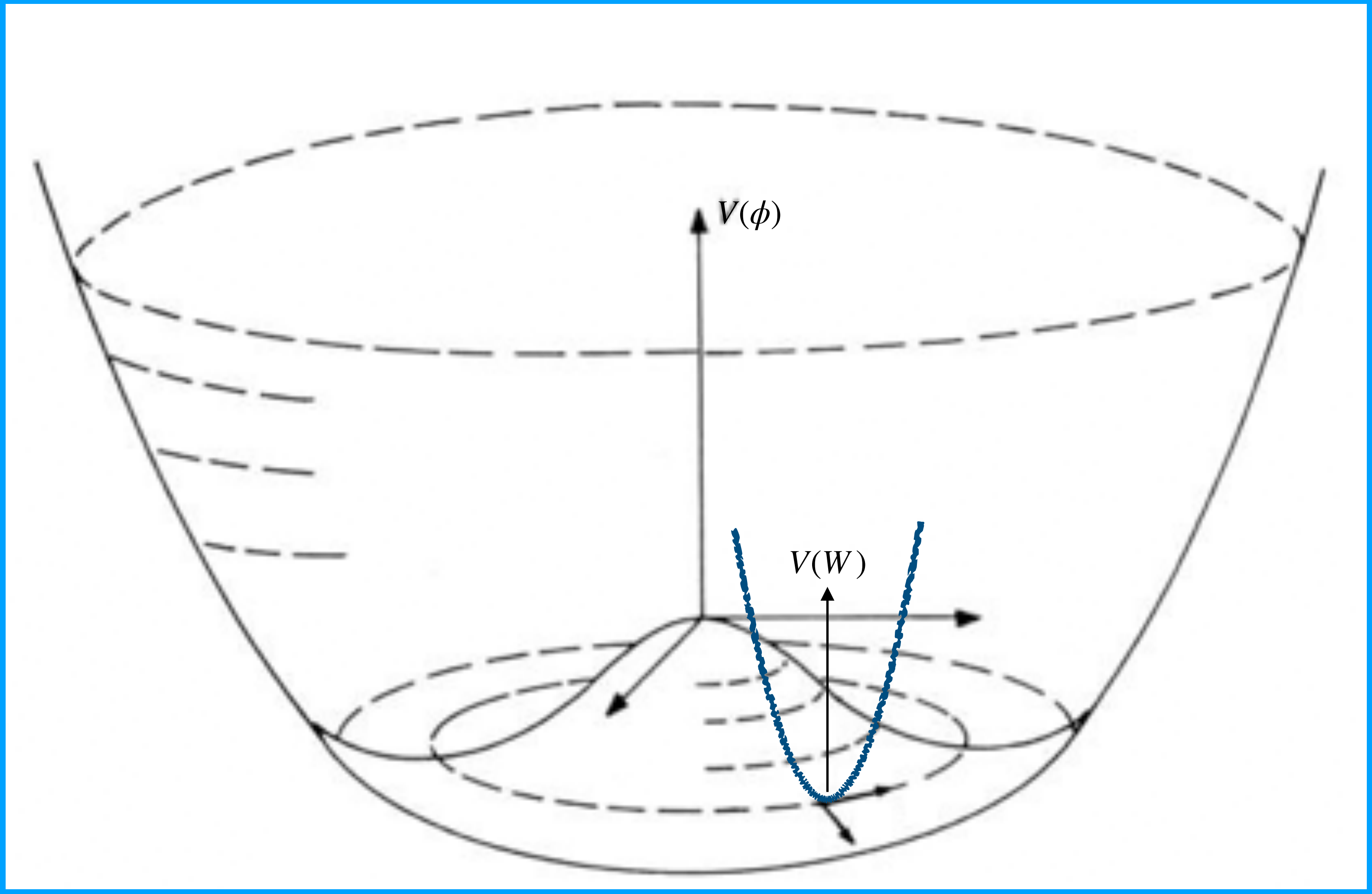

$m_H = v\sqrt{2\lambda} = 125$ GeV

$\lambda \approx 0.1$

Gauge field potential

$$V = -\frac{g^2v^2}{8}[(W^+_\mu)^2 + (W^-_\mu)^2]$$

$$-\frac{v^2(g^2+g'^2)}{8}Z^\mu Z_\mu$$

$$m_W = \frac{v}{2}g$$

$$m_Z = \frac{v}{2}\sqrt{g^2+g'^2}$$

$v = 246$ GeV and $g = 0.64$:

$m_W = 78.7$ GeV

W boson mass

Gauge quantum corrections

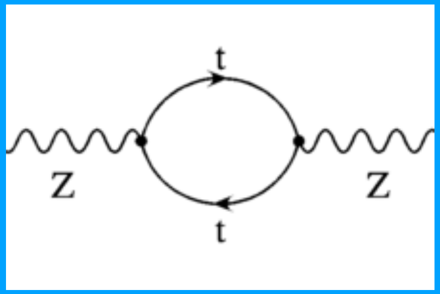

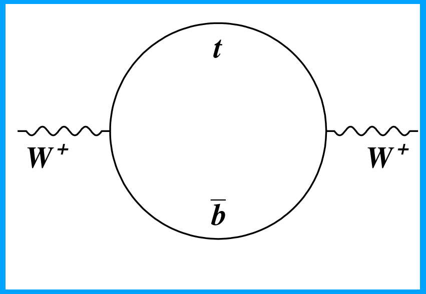

SM calculation: 81358 MeV

Higgs quantum corrections

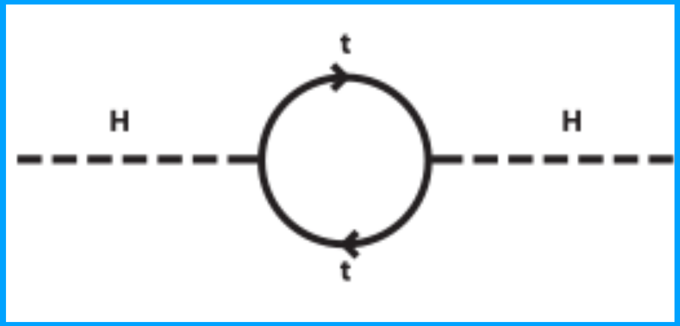

Add supersymmetry

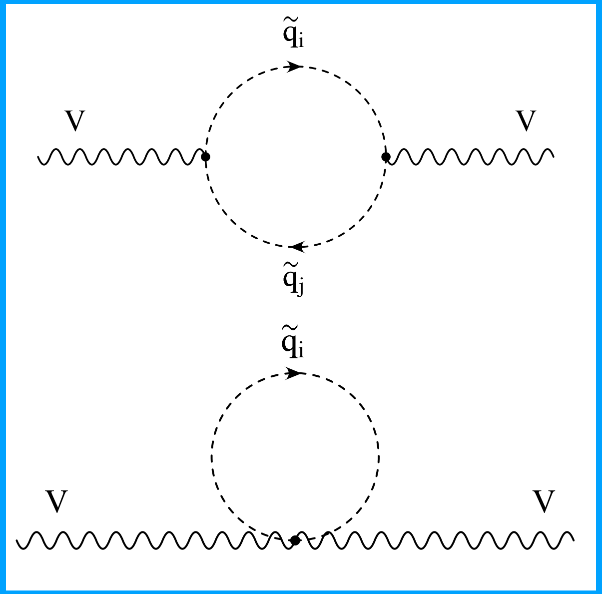

Naively integrating to a cutoff scale Λ:

$$\Delta m_H^2 = \frac{3g^2 m_t^2}{16\pi^2 m_W^2}\Lambda^2$$

If there is no new physics up to scale Λ then we need 'fine-tuning' to cancel the quantum corrections

1% fine tuning: $\Lambda = 6.6$ TeV

Motivates TeV-scale new physics

W boson mass

The SM effective field theory parameterizes general high-scale effects

$$\mathcal{L}_{SMEFT} = \mathcal{L}_{SM} + \mathcal{L}^{(5)} + \mathcal{L}^{(6)} + \mathcal{L}^{(7)} + \cdots, \qquad \mathcal{L}^{(d)} = \sum_{i=1}^{n_d} \frac{C_i^{(d)}}{\Lambda^{d-4}} Q_i^{(d)} \quad \text{for } d > 4.$$

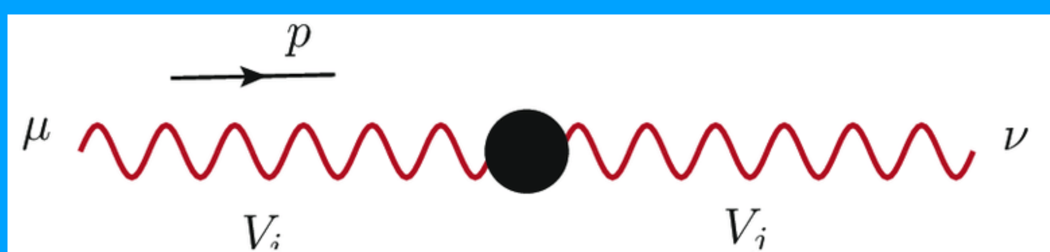

$$\frac{\delta m_W}{m_W} = \left(0.34 c_{HD} + 0.72 c_{HWB} + 0.37 c_{Hl3} - 0.19 c_{ll1}\right) \frac{v^2}{\Lambda^2}$$

For $\delta m_W / m_W = 0.1\ \%$ and c_{HD}=1, $\Lambda = 4.5$ TeV

e.g. Z' boson

For $\delta m_W / m_W = 0.1\ \%$ and c_{HWB}=1, $\Lambda = 6.6$ TeV

e.g. compositeness

Smaller $c_i \rightarrow$ smaller Λ

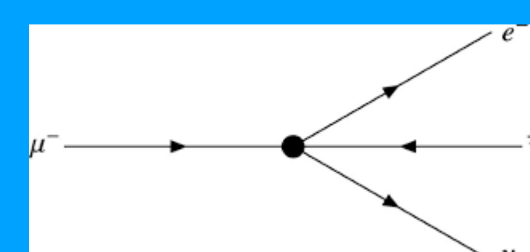

CDF @ Tevatron

$\sqrt{s} = 1.96$ TeV proton-antiproton collisions from the Fermilab Tevatron

CDF: 8.8 fb^{-1} of integrated luminosity

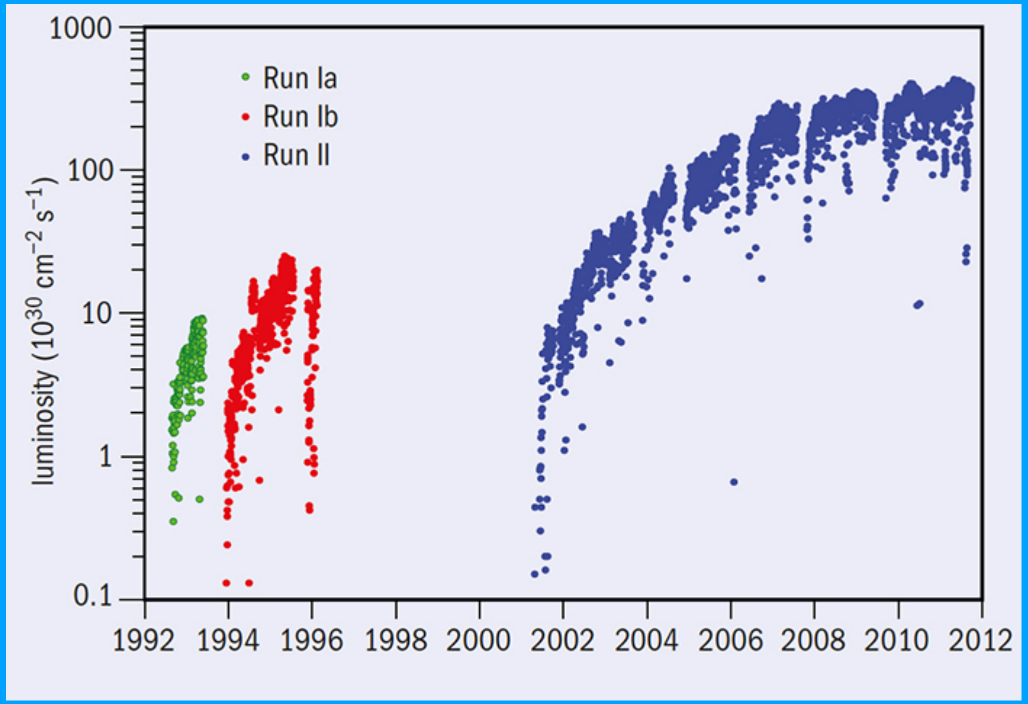

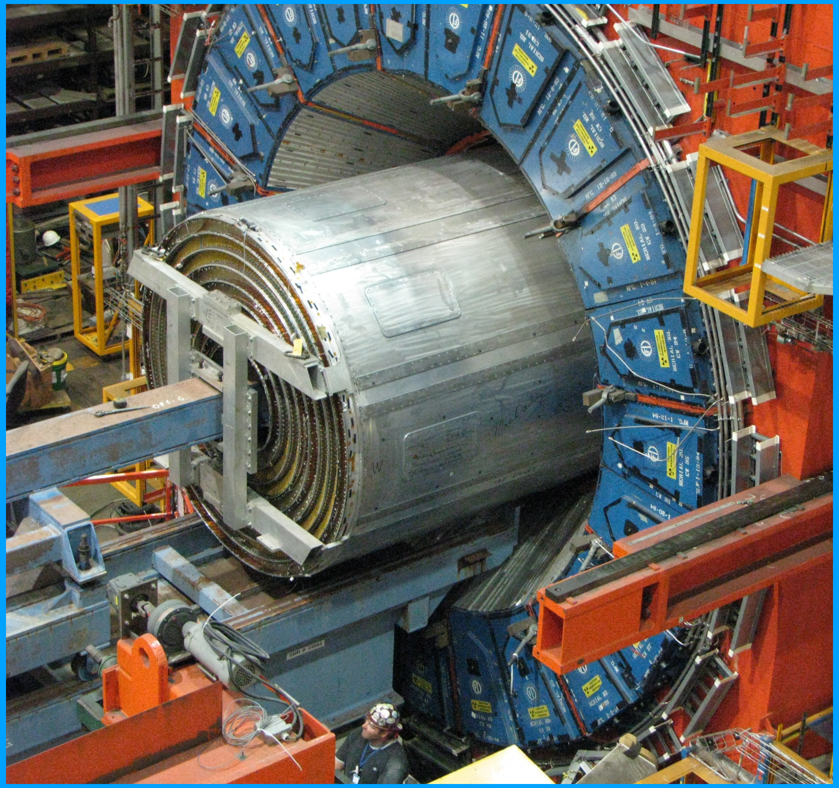

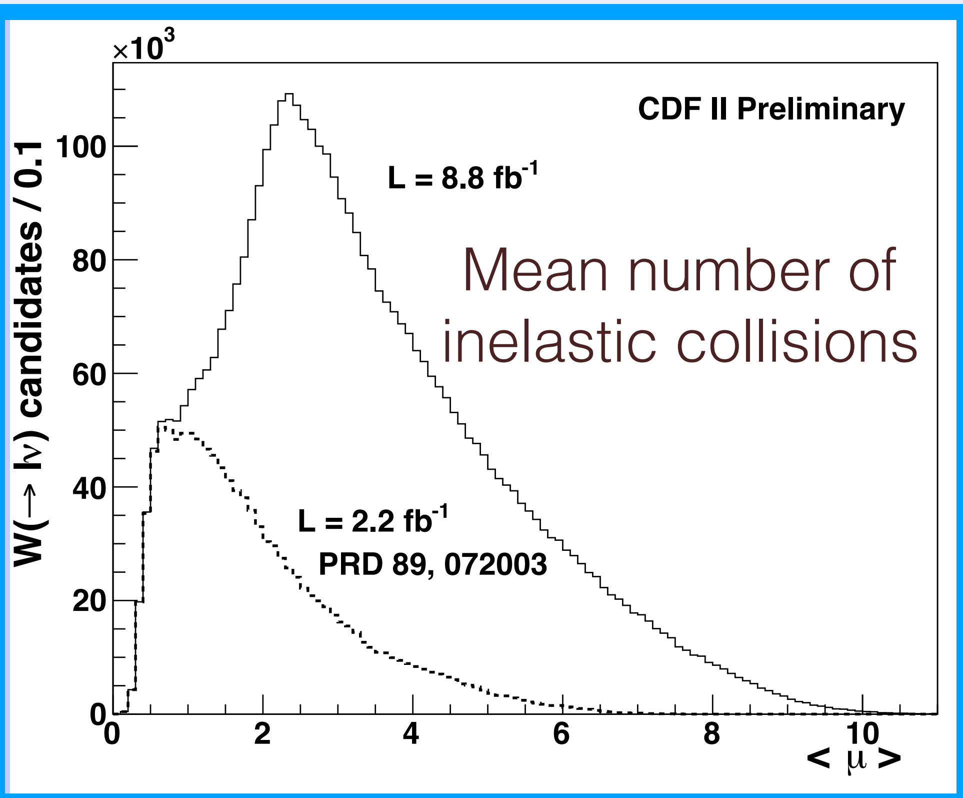

Measurement overview

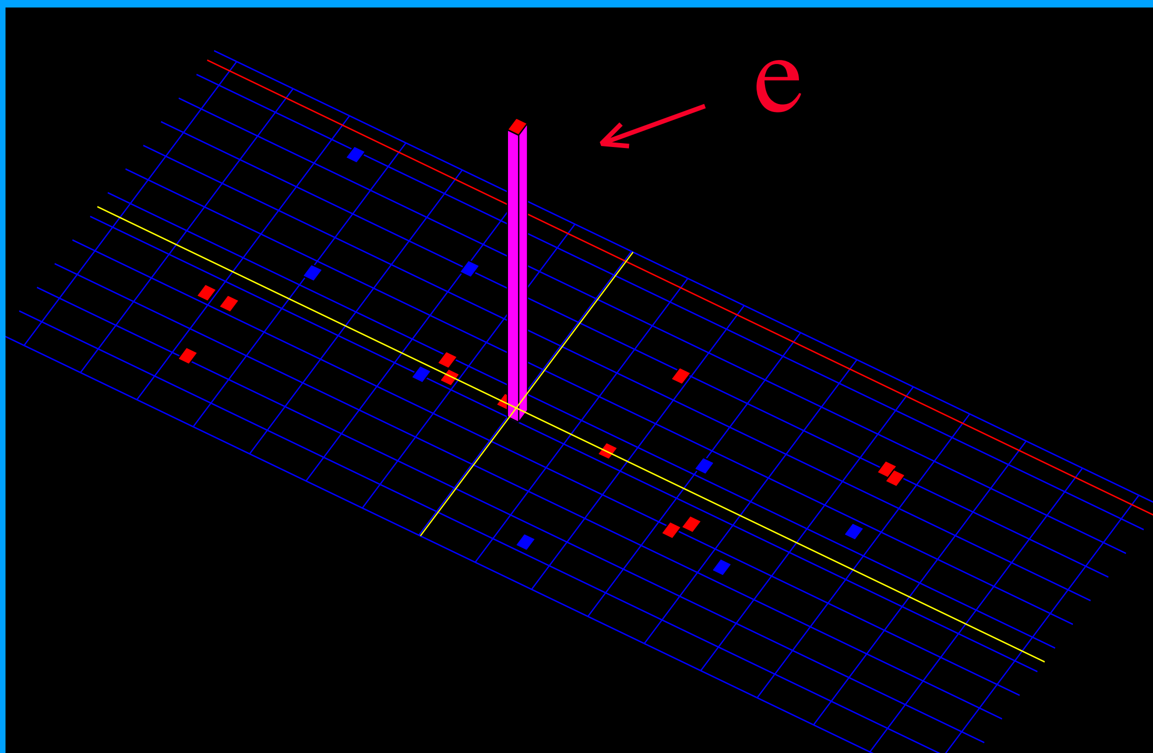

W bosons identified in their decays to $e\nu$ and $\mu\nu$

Mass measured by fitting template distributions of transverse momentum and mass

$$m_T = \sqrt{2p_T^l \not{p}_T \,(1 - \cos\Delta\phi)}$$

$$\vec{\not{p}}_T = -(\vec{p}_T^{\,l} + \vec{u}_T)$$

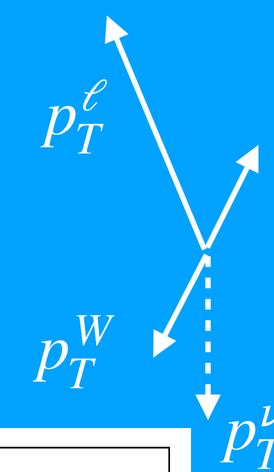

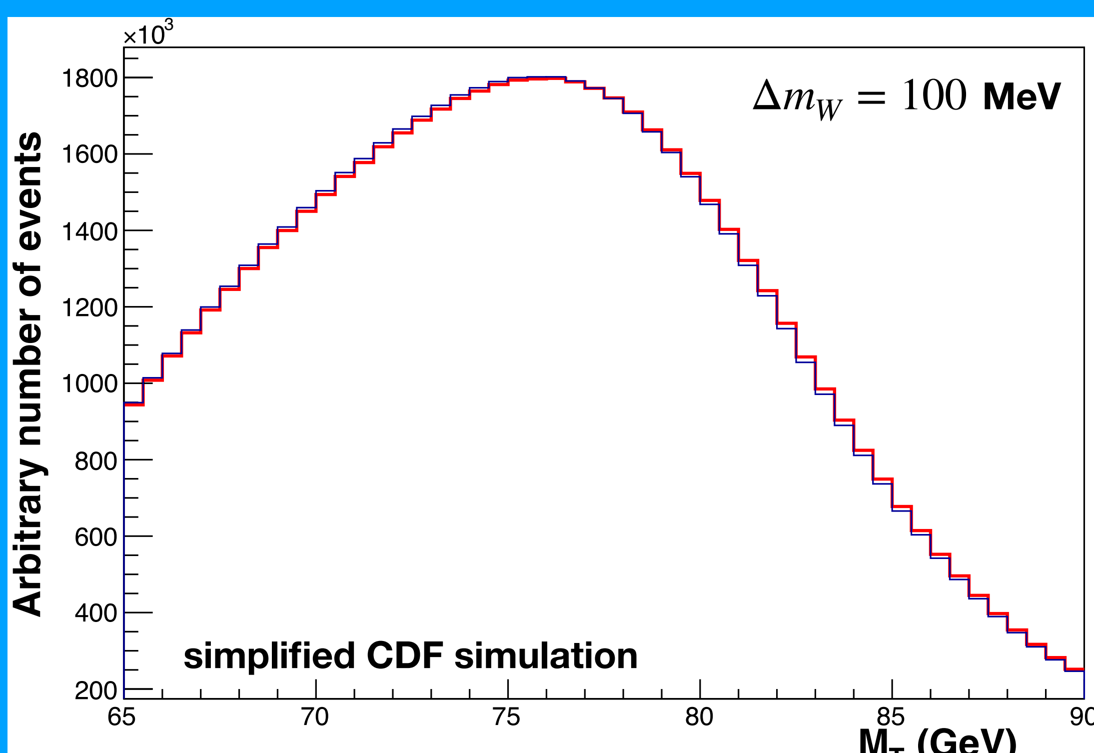

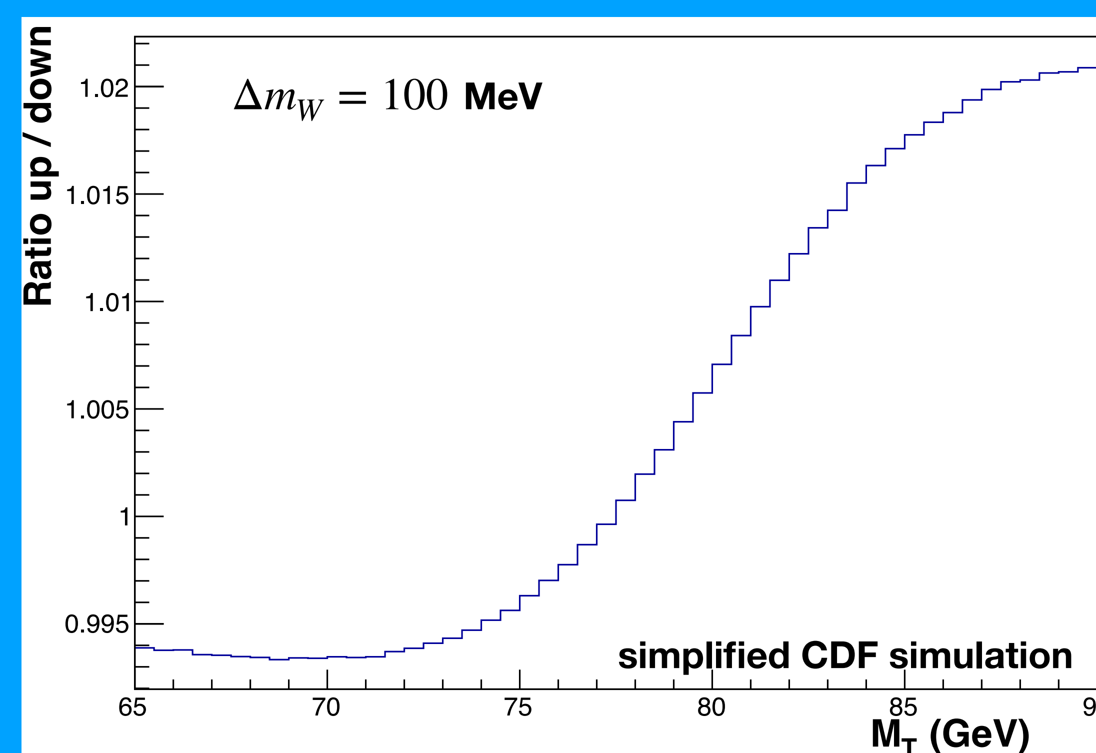

Calibrations

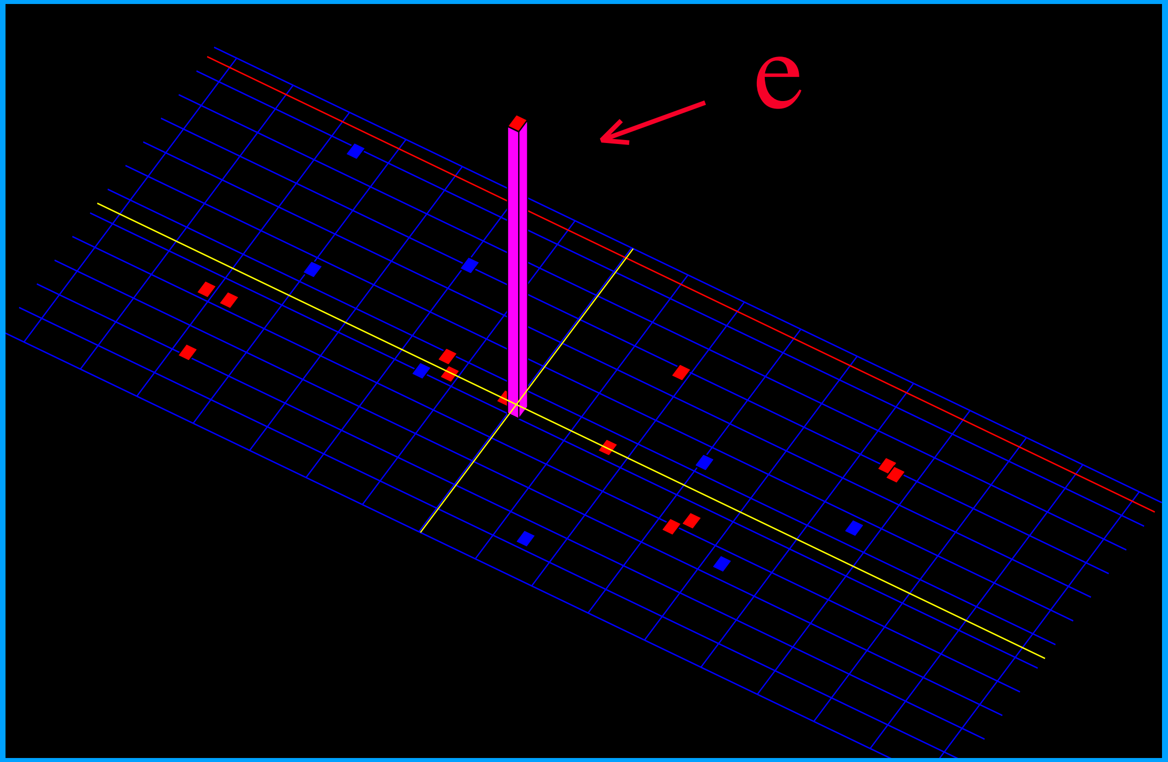

W bosons identified in their decay to $e\nu$ or $\mu\nu$

Measurement requires precise calibrations of momentum scale and resolution

Charged lepton scale:

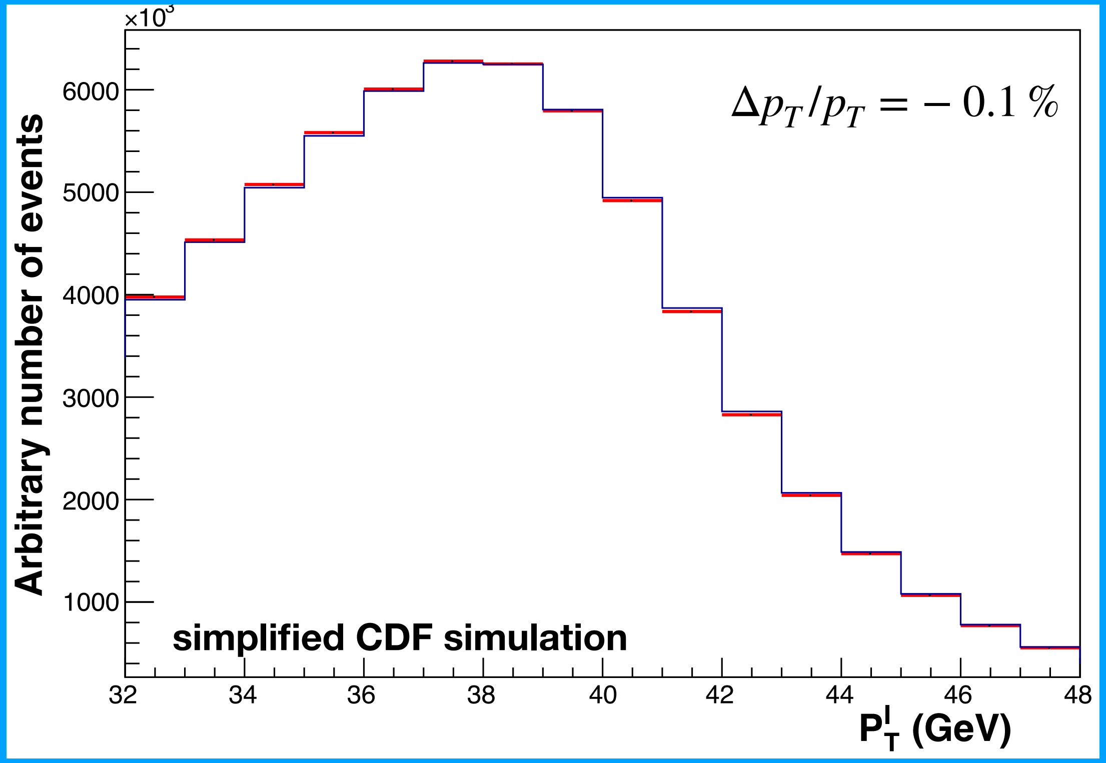

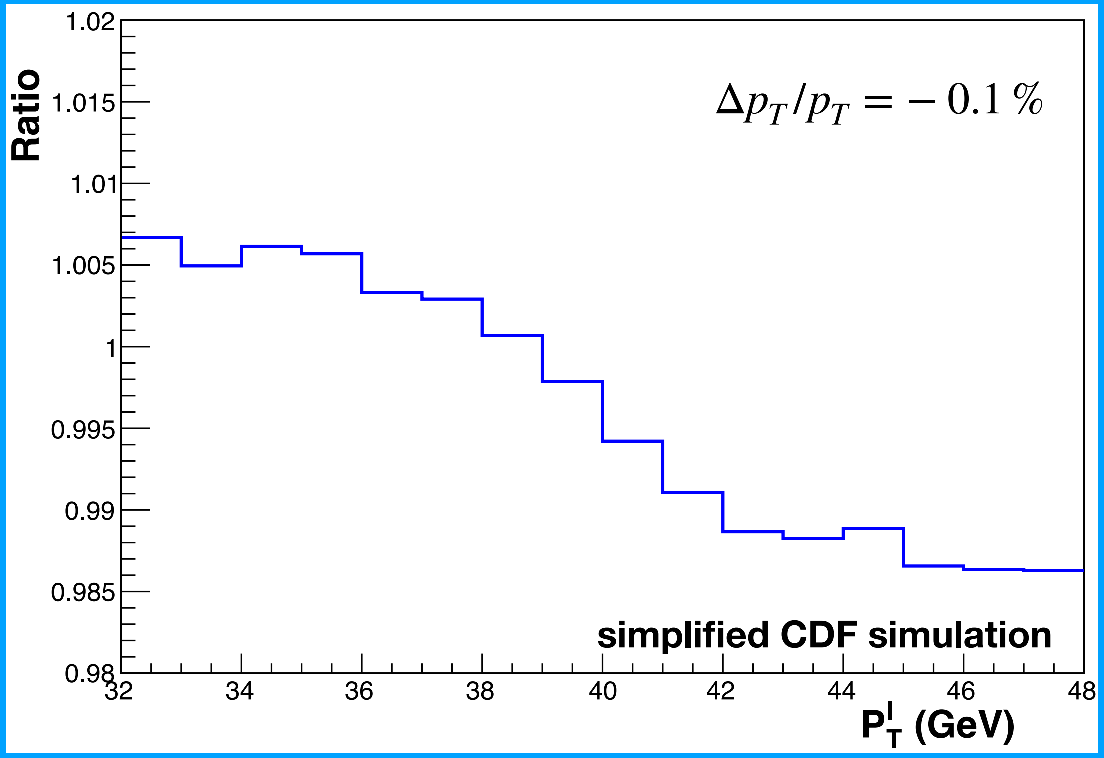

Muon momentum calibration

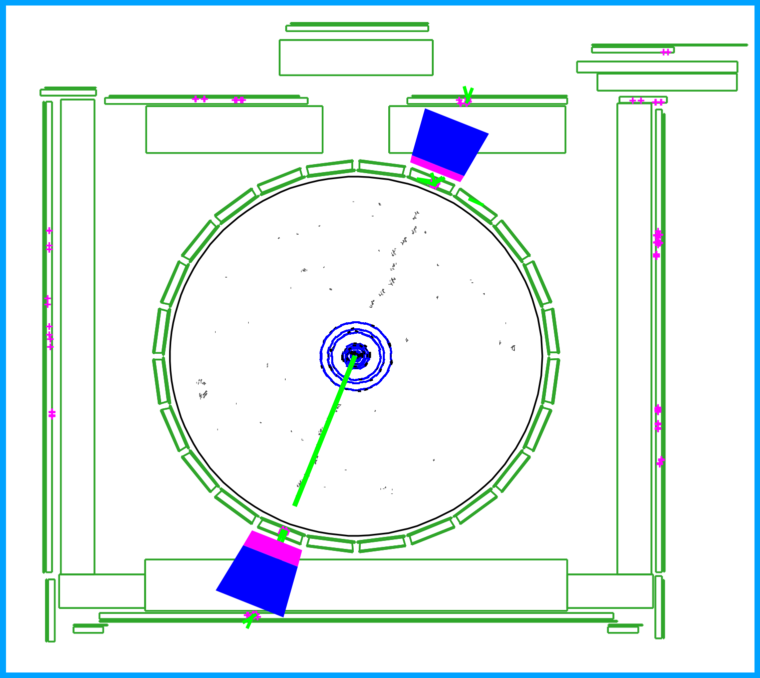

First step is to align the tracker system

Determine individual 'sensor' positions by minimizing χ^2 difference between sensor and reconstructed track positions using cosmic-ray and collision data

CDF: 10k drift-chamber degrees of freedom
(shift & rotation for each of 2520 cells at each endplate)

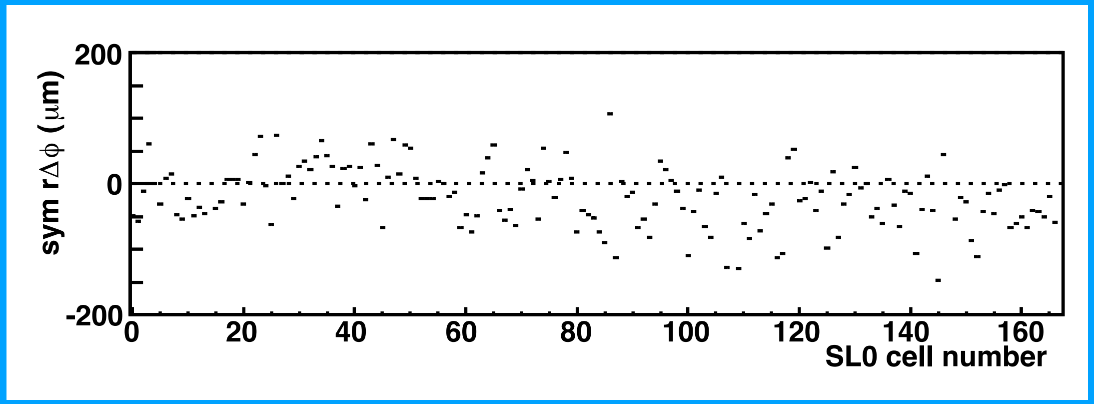

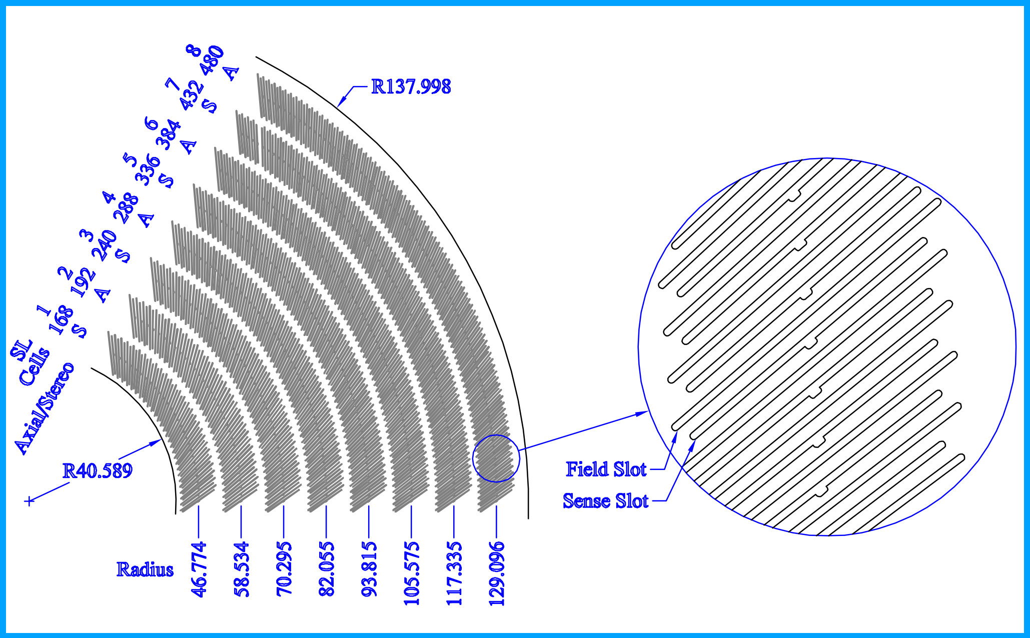

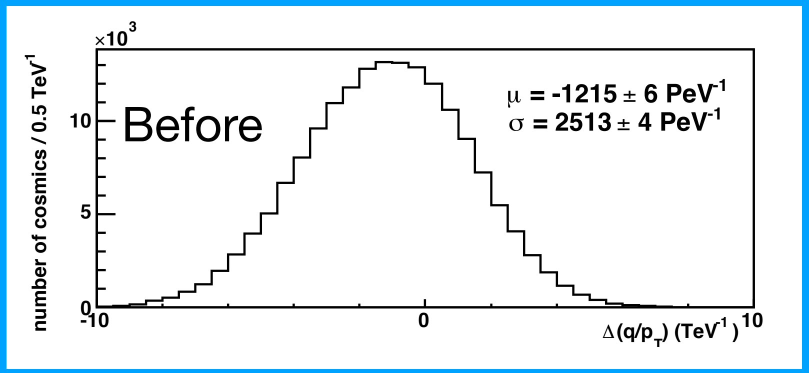

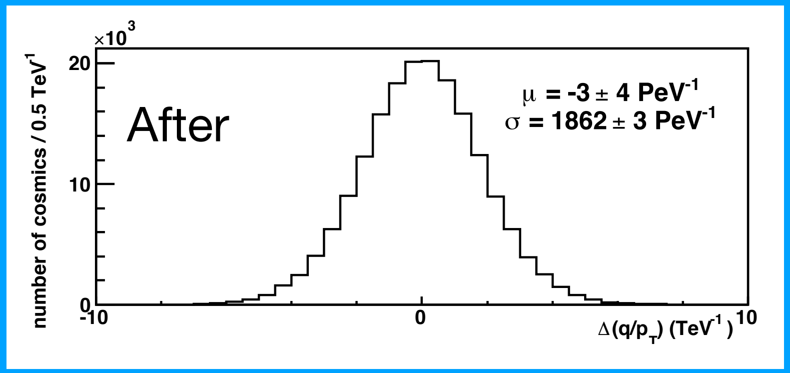

Kotwal & CH, NIMA 762, 85 (2014)

Muon momentum calibration

Second step is to correct for biases unconstrained by alignment procedure

Use data from resonance decays to muons and electrons

Correct curvature as function of polar angle using electrons from $W \rightarrow e\nu$ and $Z \rightarrow ee$ decays

Use J/ψ, Υ, and Z decays to correct for tracker length, field nonuniformities, endplate twists, and amount of material upstream of drift chamber

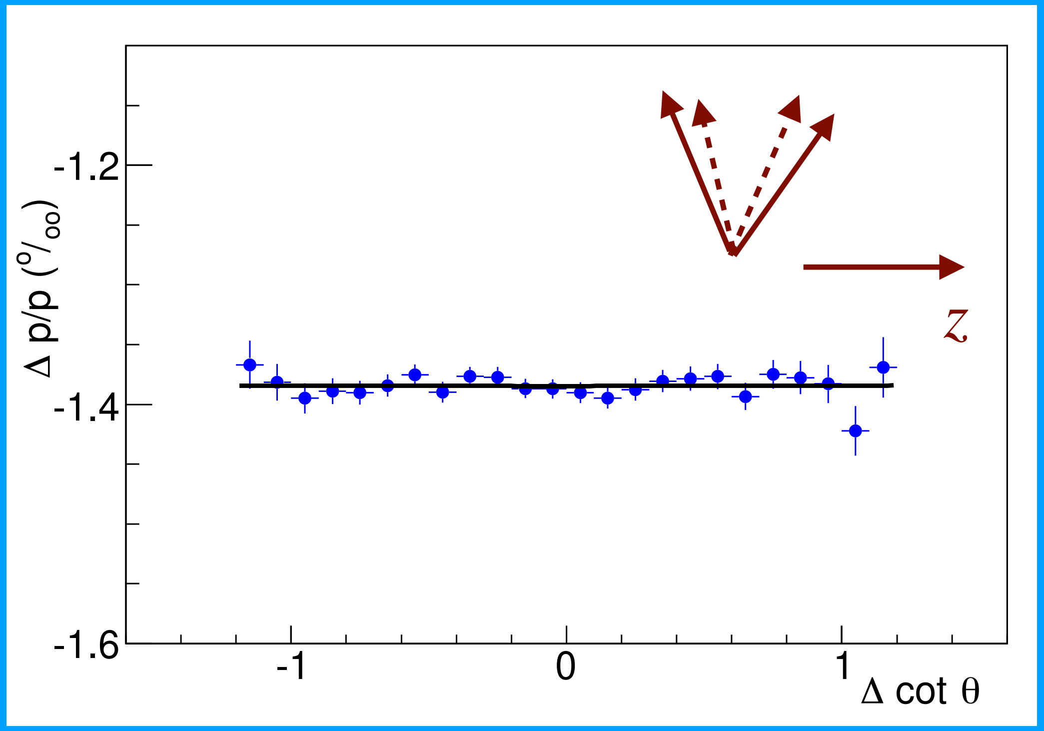

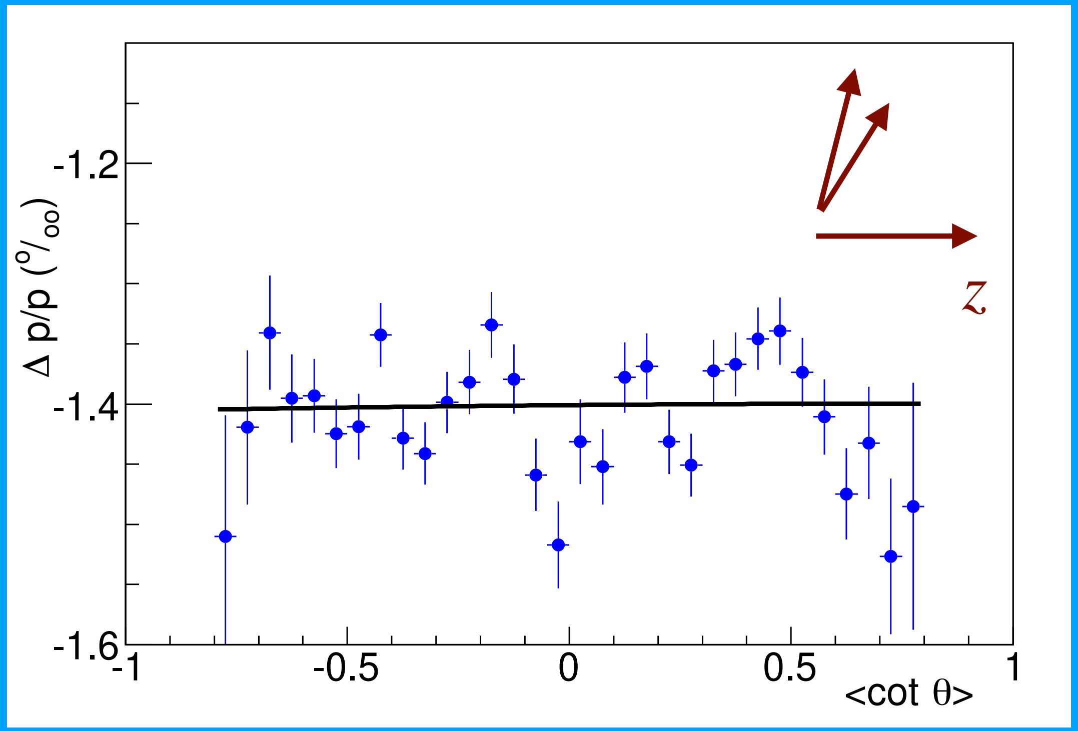

Muon momentum calibration

Third step is to calibrate the momentum scale using J/ψ, Υ, and Z decays to muons

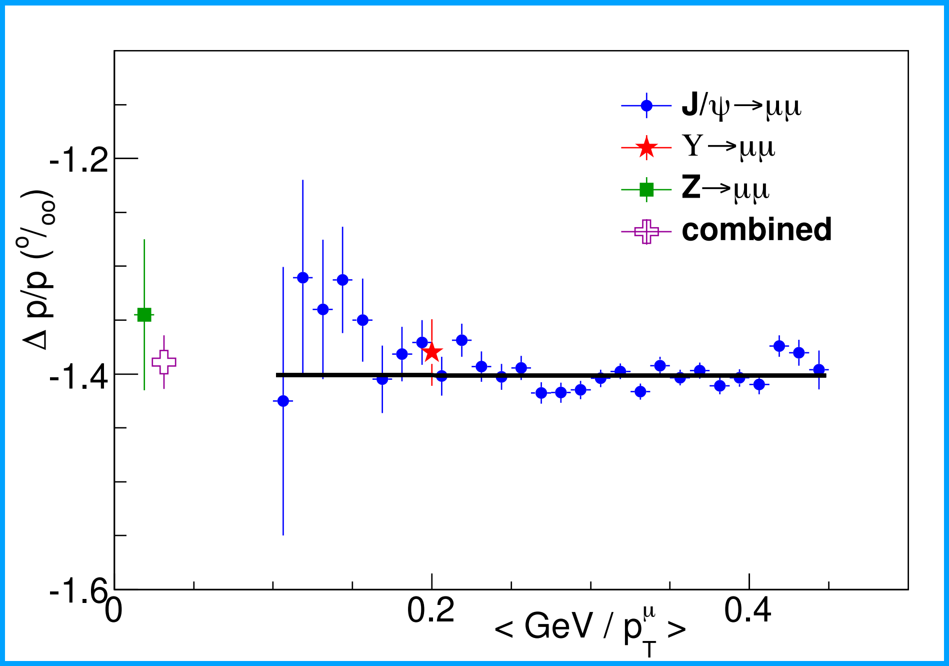

Z boson mass in the muon decay channel is measured to be

$$M_Z = 91\ 192.0 \pm 6.4_{stat} \pm 4.0_{sys}\ \text{MeV}$$

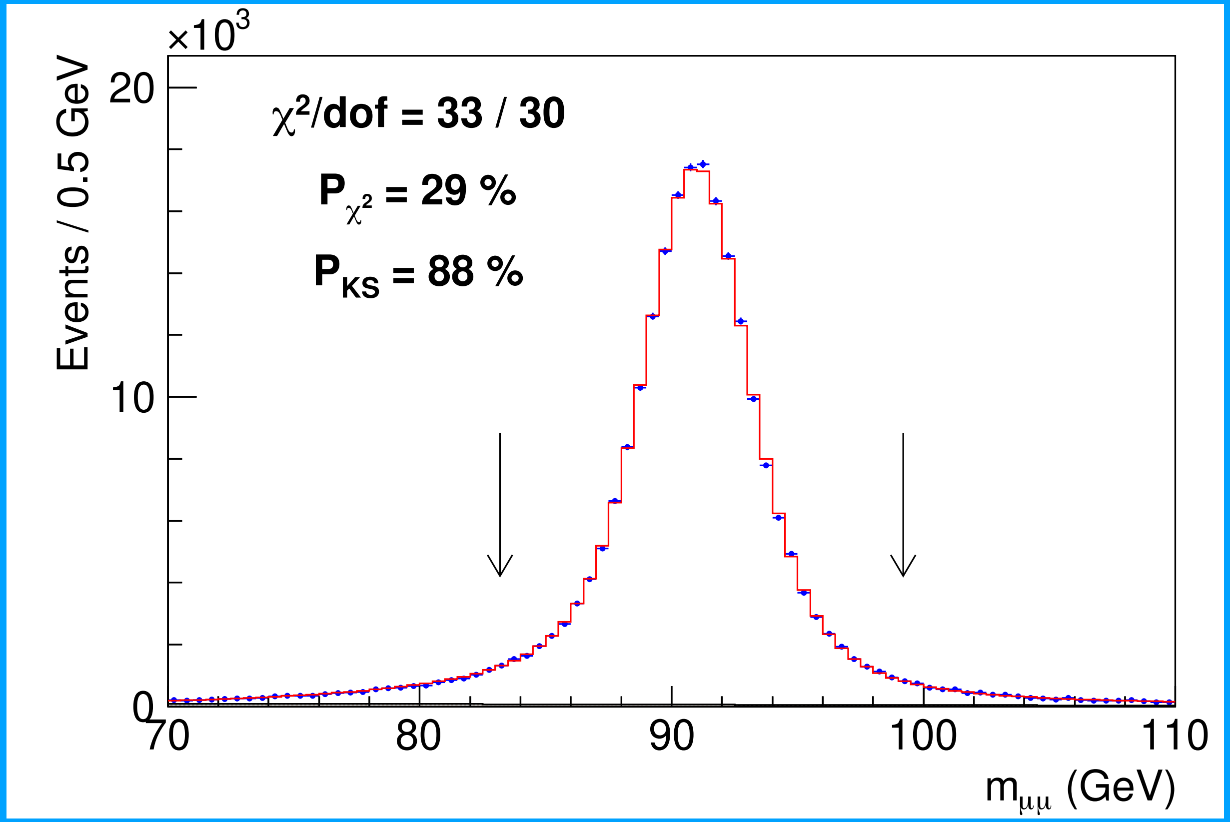

The most precise measurement of the Z boson mass at a hadron collider

Uncertainty is 3.6 times that of LEP

Electron momentum calibration

First step is to correct the response variations in data

Use ratio of calorimeter energy to track momentum (E/p) to remove response variations with time and position within tower and in pseudorapidity

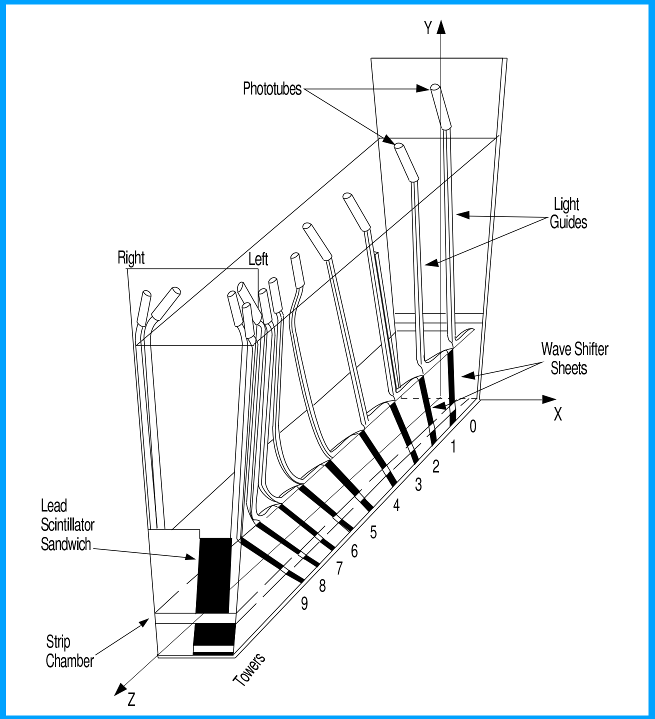

Second step is to simulate the energy loss

Tune the amount of upstream material using E/p from $W \to e\nu$ events
Correct the downstream energy leakage using E/p

Tower	Thickness (x_0)	Number of lead sheets
0	17.9	30
1	18.2	30
2	18.2	29
3	17.8	27
4	18.0	26
5	17.7	24
6	18.1	23
7	17.7	21
8	18.0	20

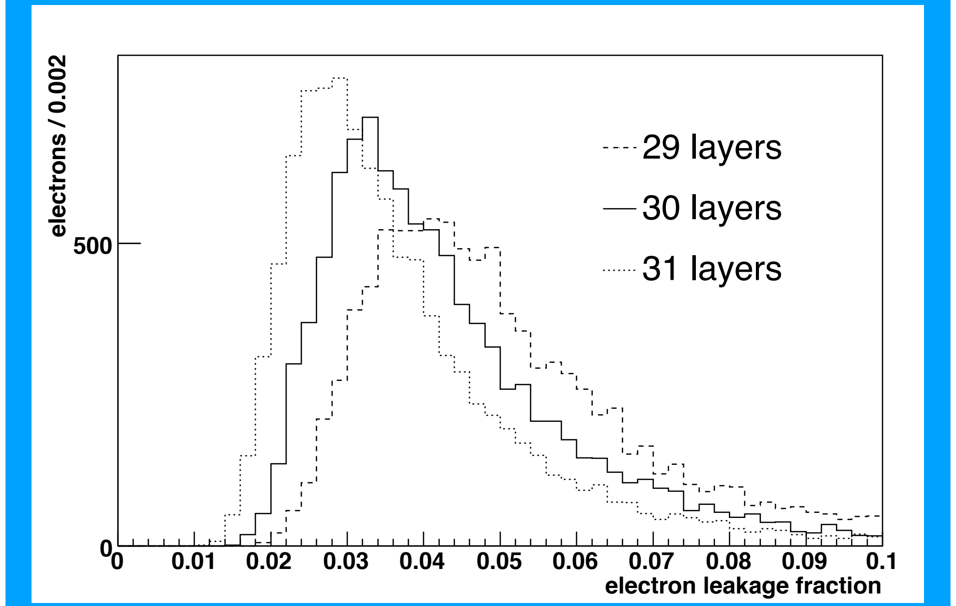

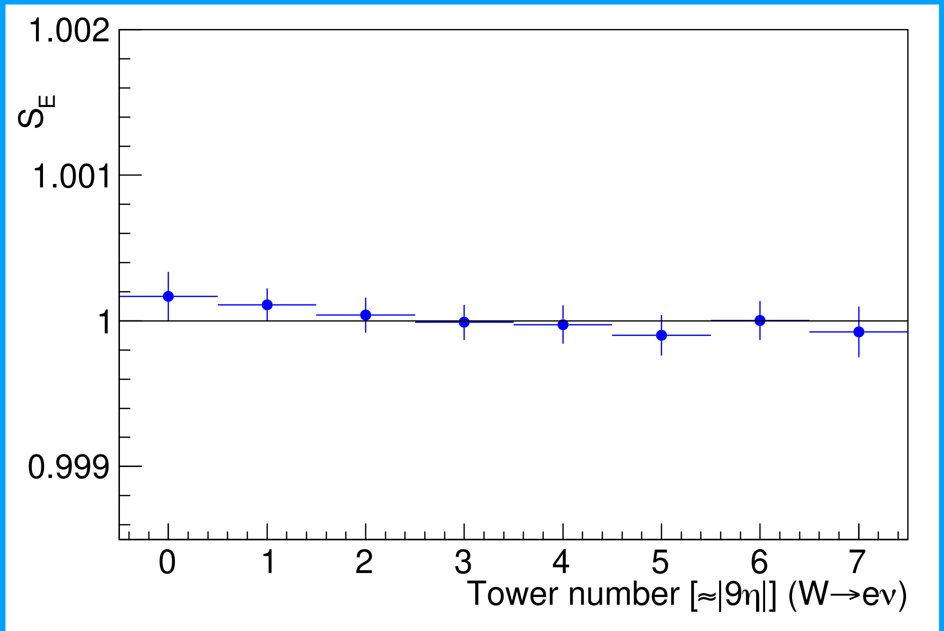

Kotwal & CH, NIMA 729, 25 (2013)

Electron momentum calibration

Third step is to calibrate the response

Transfer track momentum calibration to calorimeter using (E/p) distribution, combine with calibration from $Z \rightarrow ee$ decays

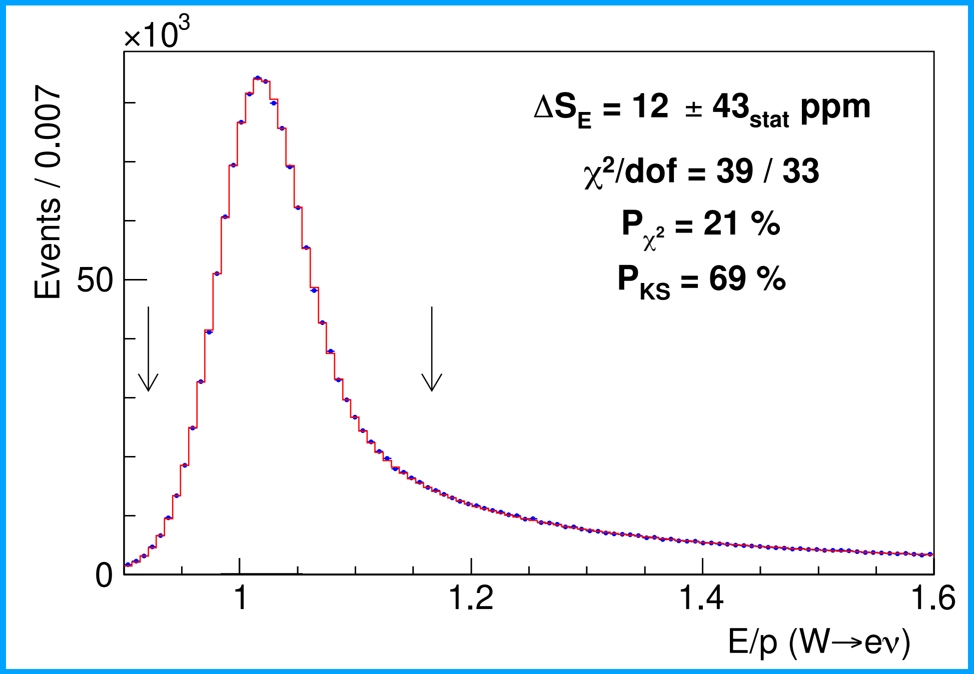

Z boson mass in the electron decay channel measured to be

$$M_Z = 91\ 194.3 \pm 13.8_{stat} \pm 7.6_{sys} \text{ MeV}$$

Consistent with measurement in muon channel

Lower precision due to calorimeter dead regions

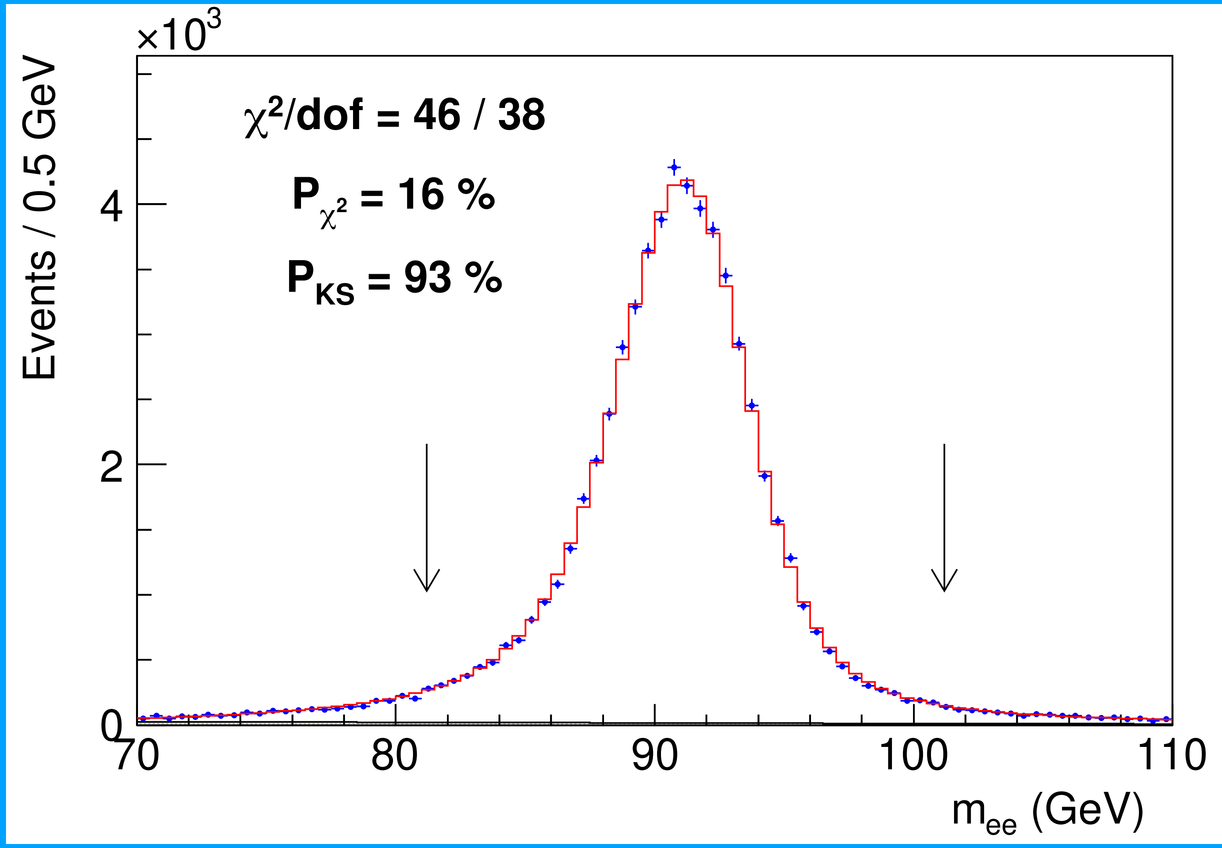

Calibrations

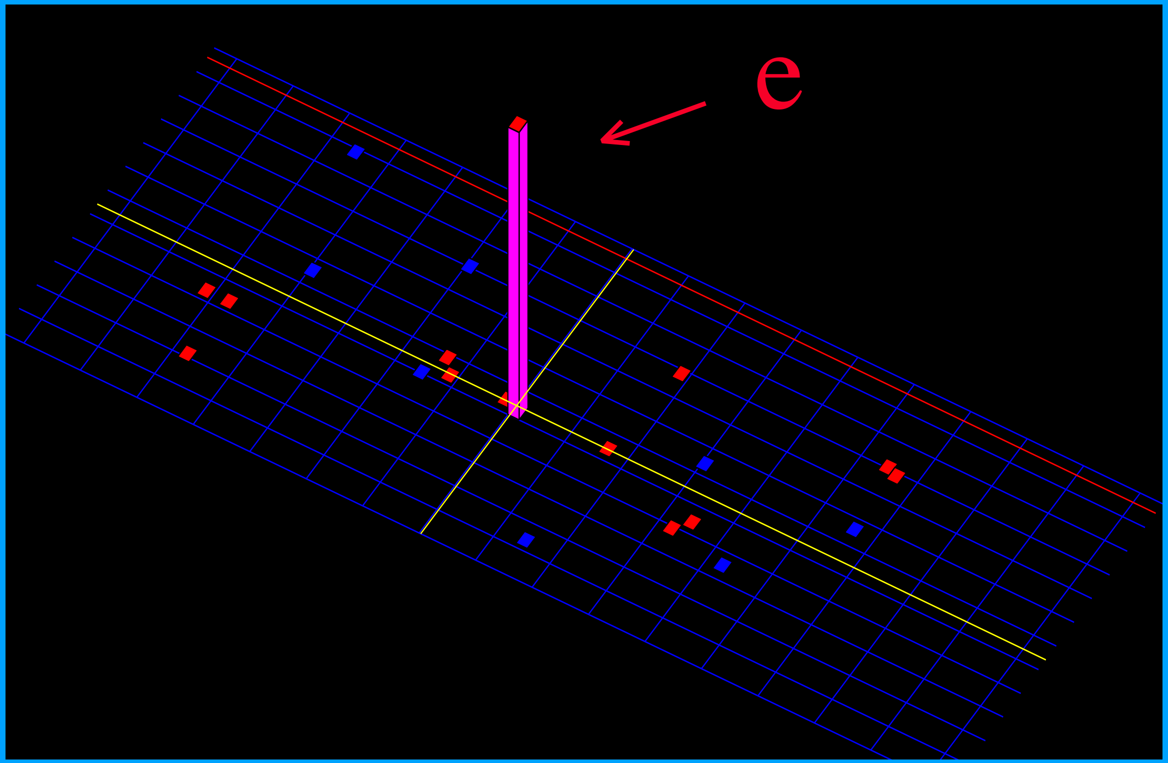

Measurement requires precise calibrations of momentum scale and resolution

$$\vec{\not{p}}_T = -(\vec{p}_T^{\,l} + \vec{u}_T)$$

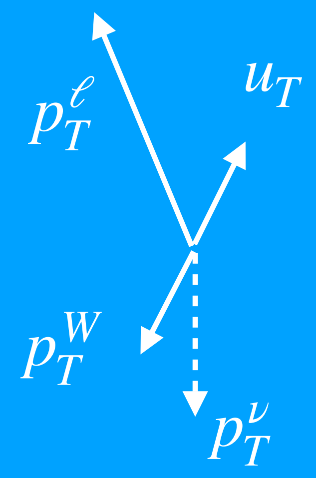

Recoil scale

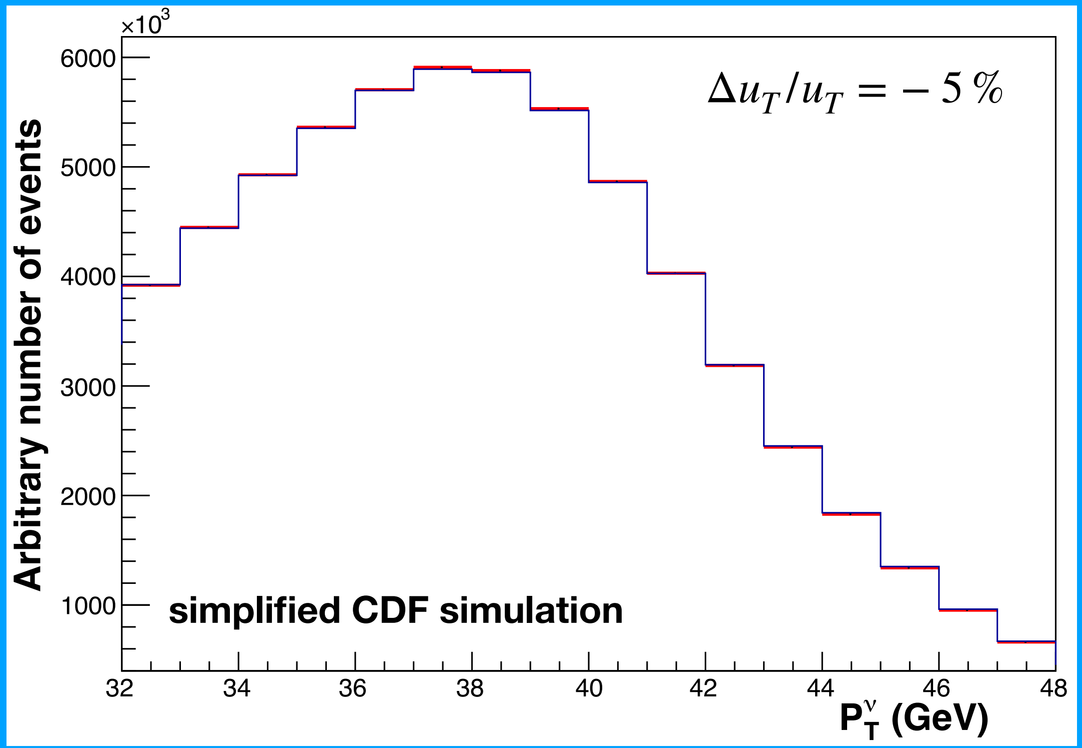

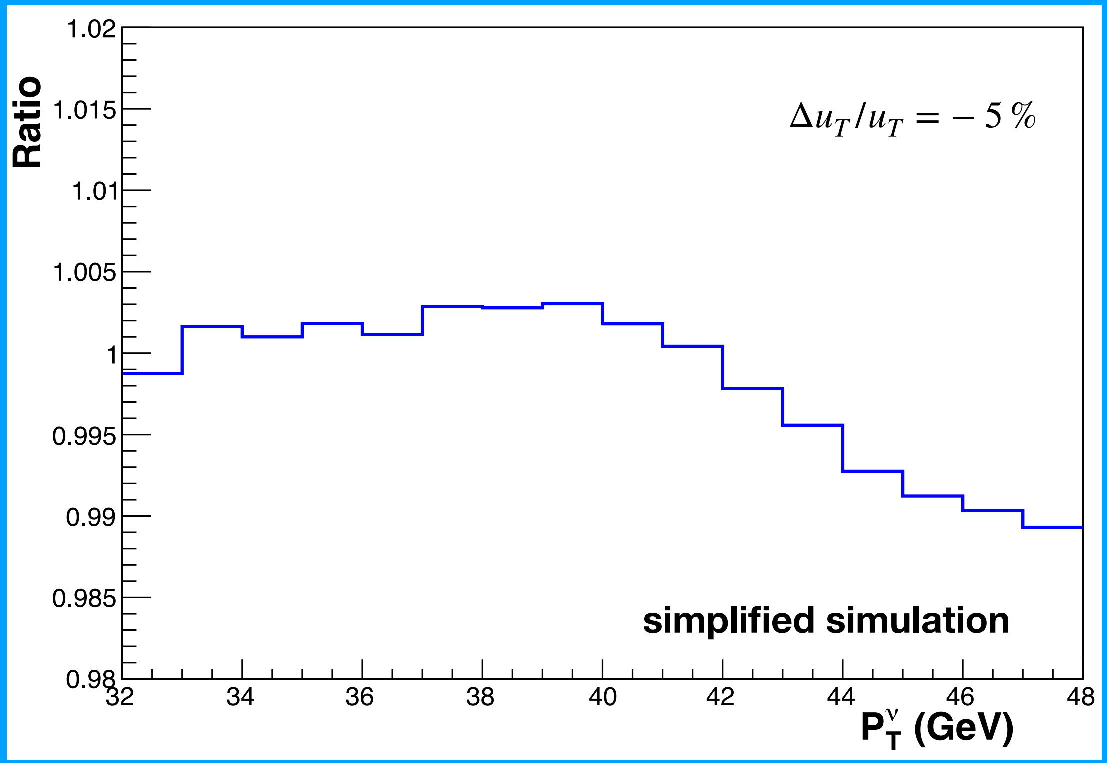

Recoil momentum calibration

First step is data uniformity corrections

Align calorimeter relative to the beam axis to remove any modulation in the recoil direction

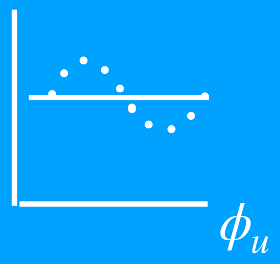

Second step is the reconstruction of the recoil

Remove custom tower windows traversed by electrons or muons

Remove corresponding recoil energy in simulation using a distribution from towers rotated by 90°

Validate the procedure by studying towers rotated by 180°

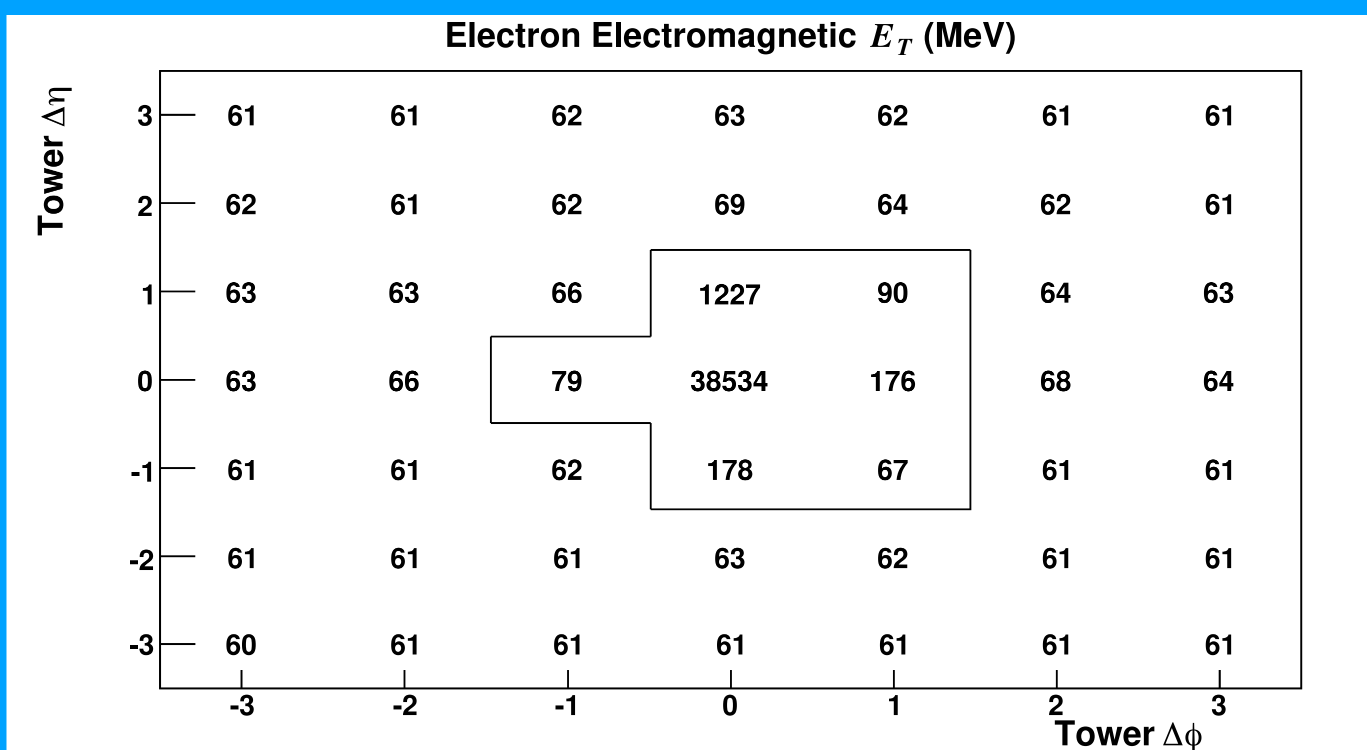

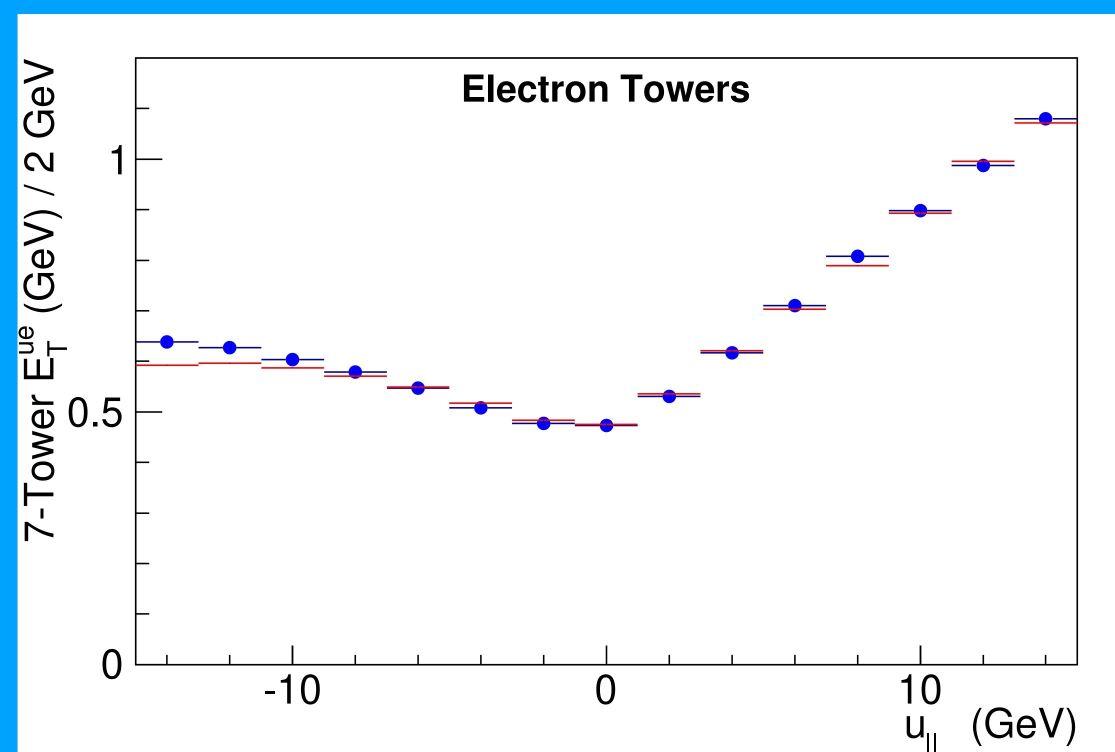

Recoil momentum calibration

Third step is the calibration of the recoil response

Scale generated recoil to balance p_T^Z and check observed response R_{rec}

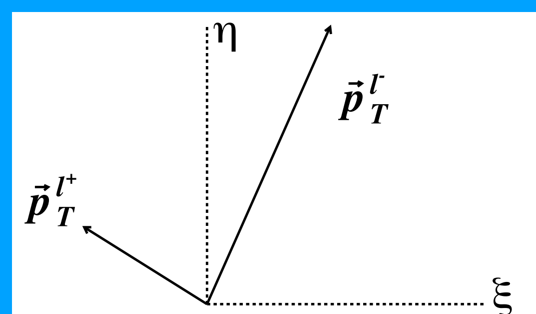

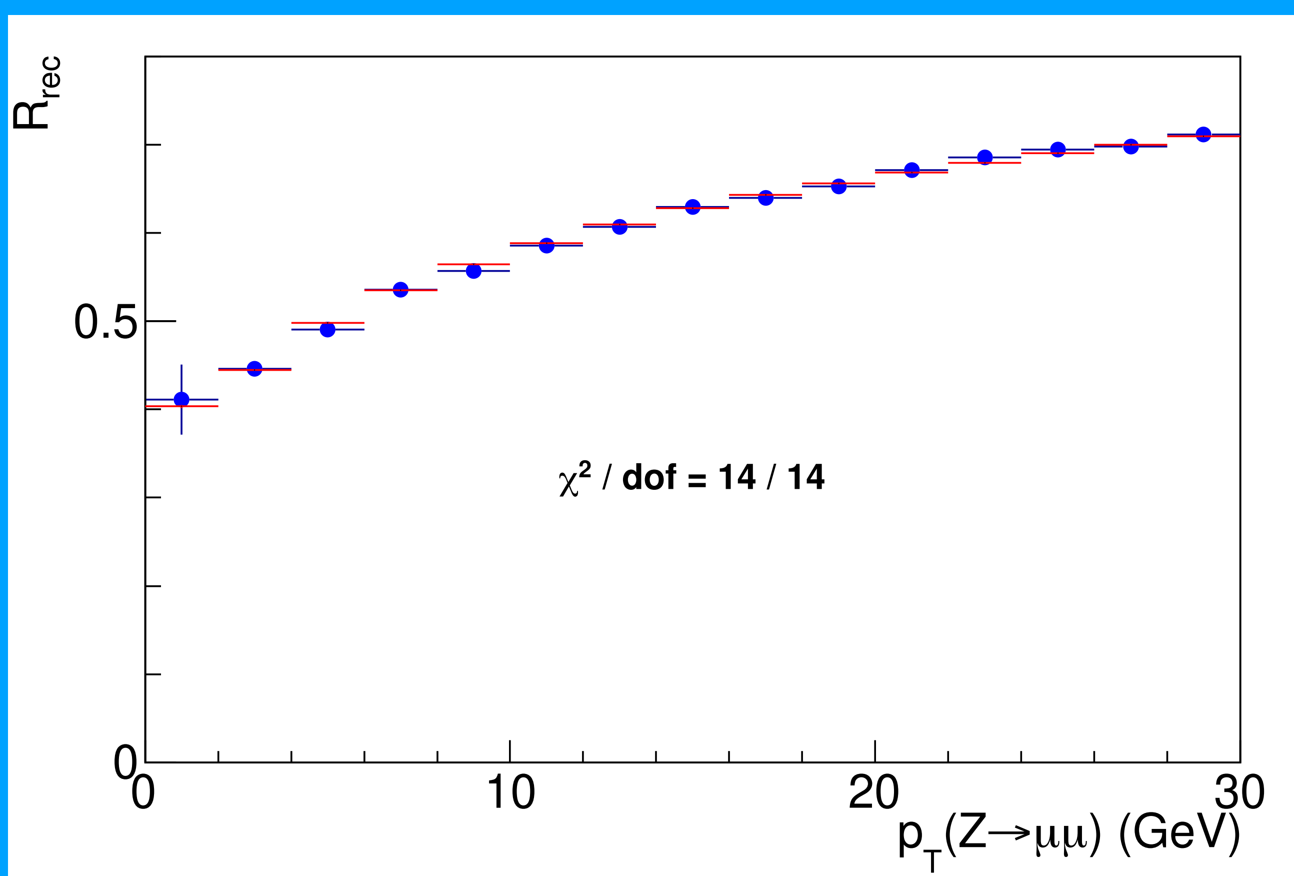

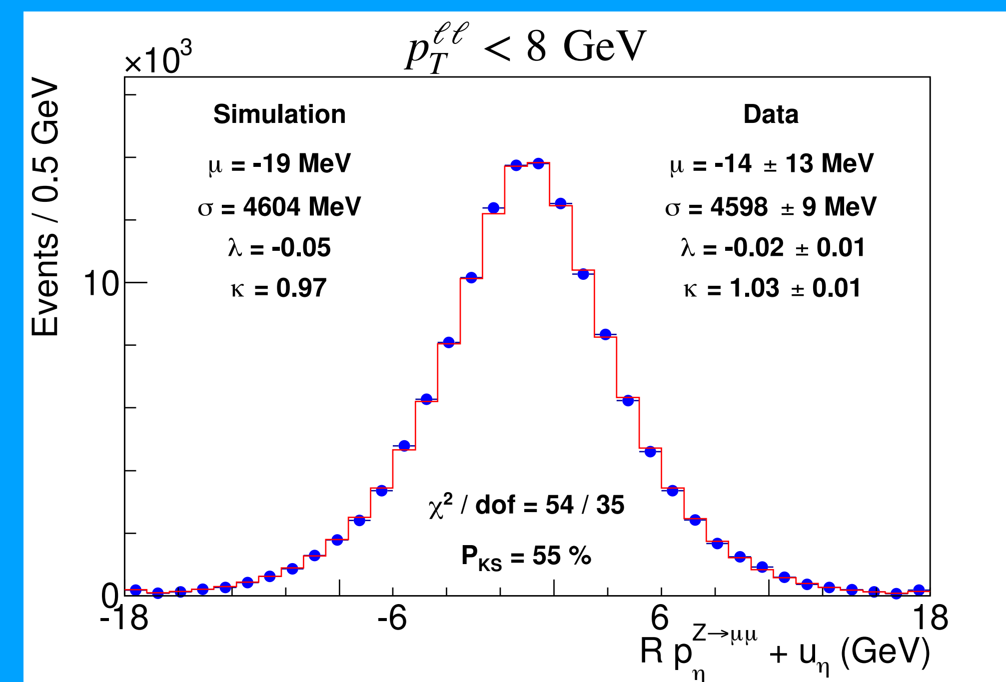

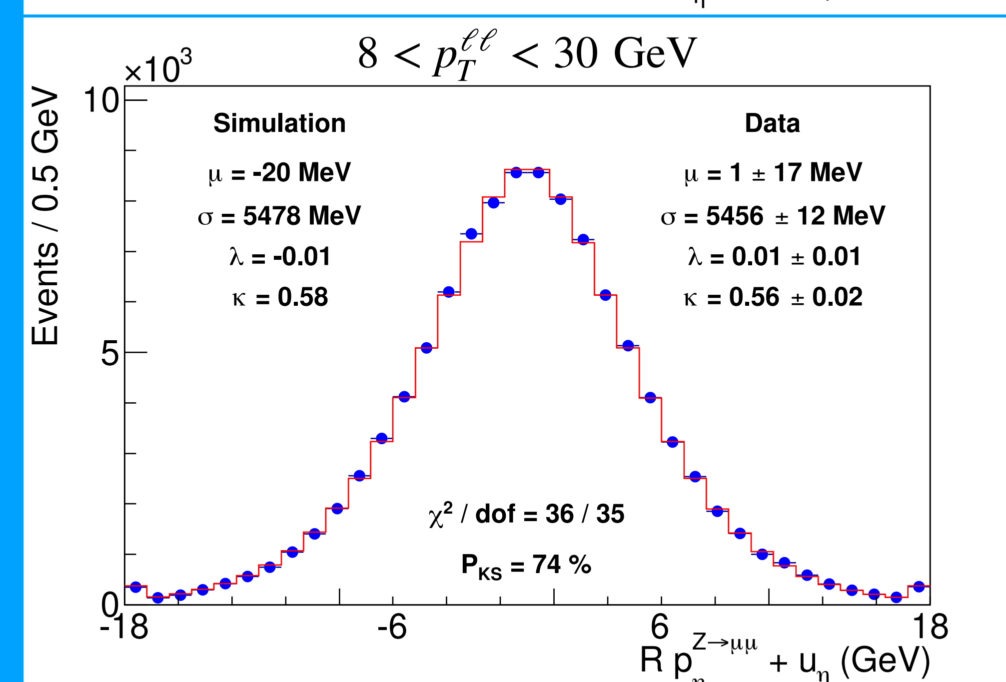

Recoil momentum calibration

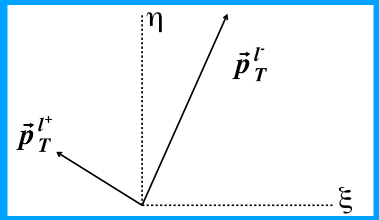

Fourth step is the calibration of the recoil resolution

Includes jet-like energy and angular resolution, additional dijet fraction term, and pileup

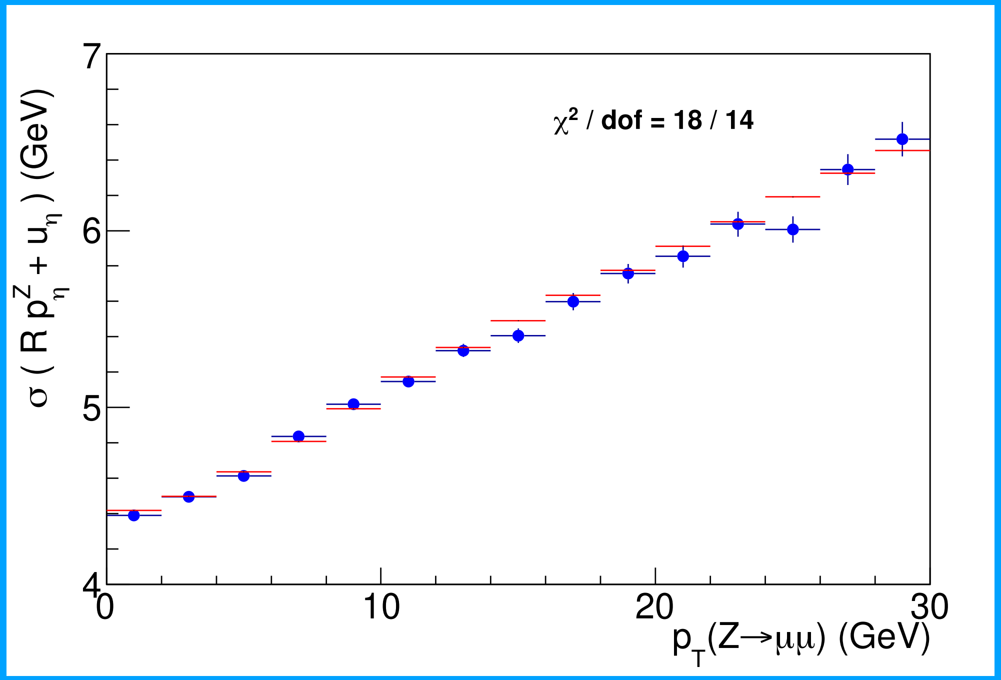

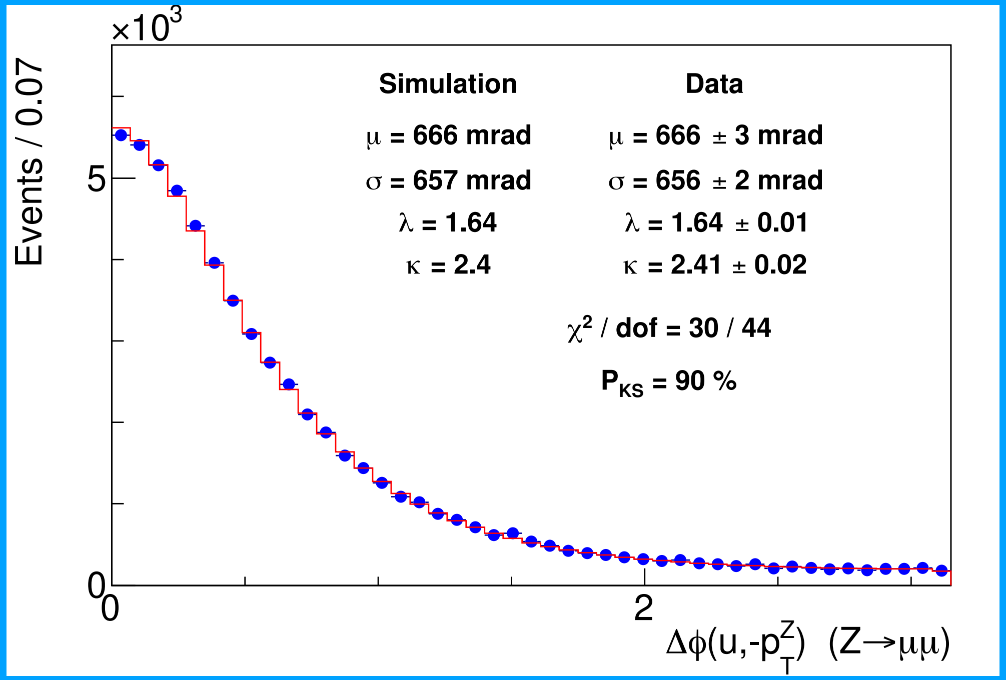

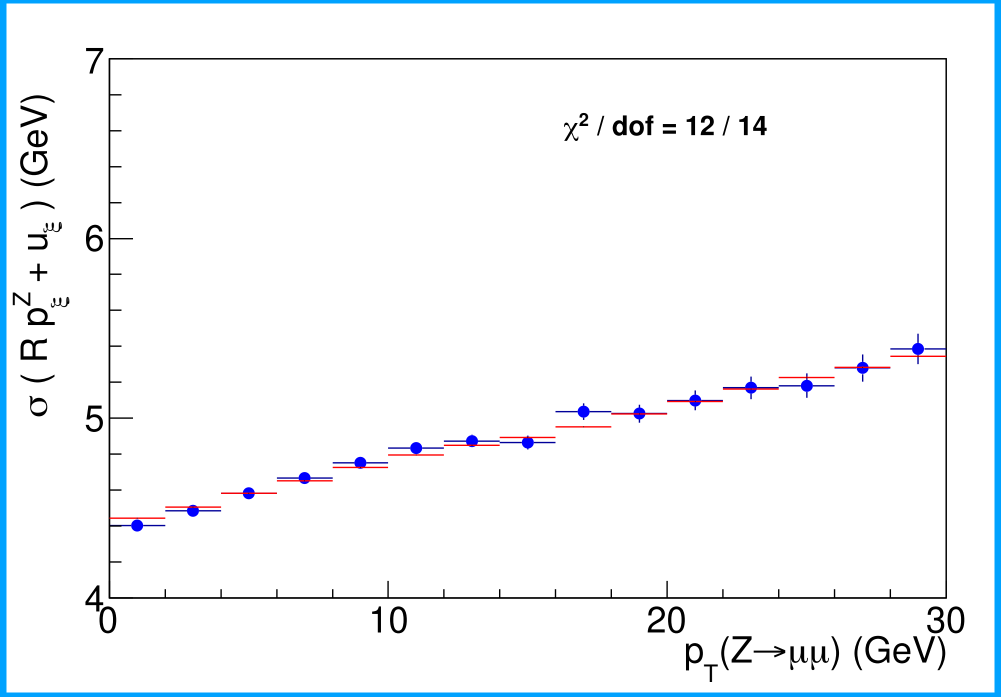

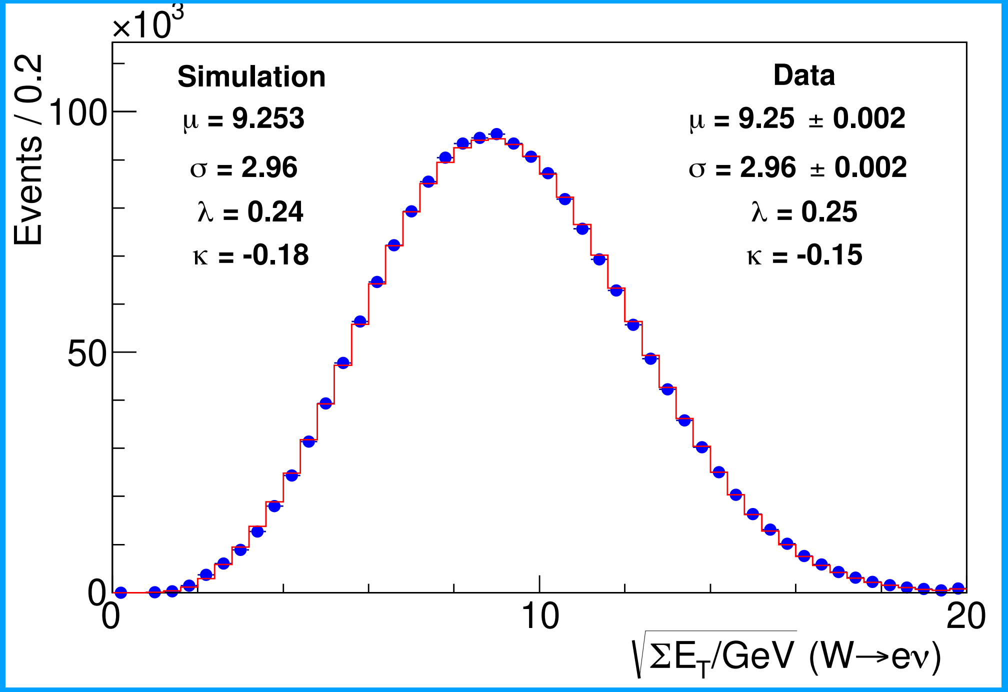

Recoil momentum validation

W boson recoil distributions validate the model

Most important is the recoil projected along the charged-lepton's momentum ($u_{||}$)

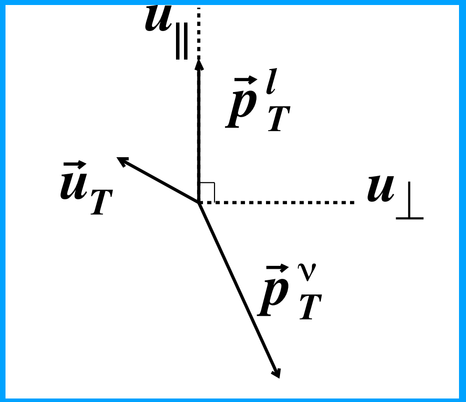

$$m_T \approx 2p_T\sqrt{1 + u_{||}/p_T} \approx 2p_T + u_{||}$$

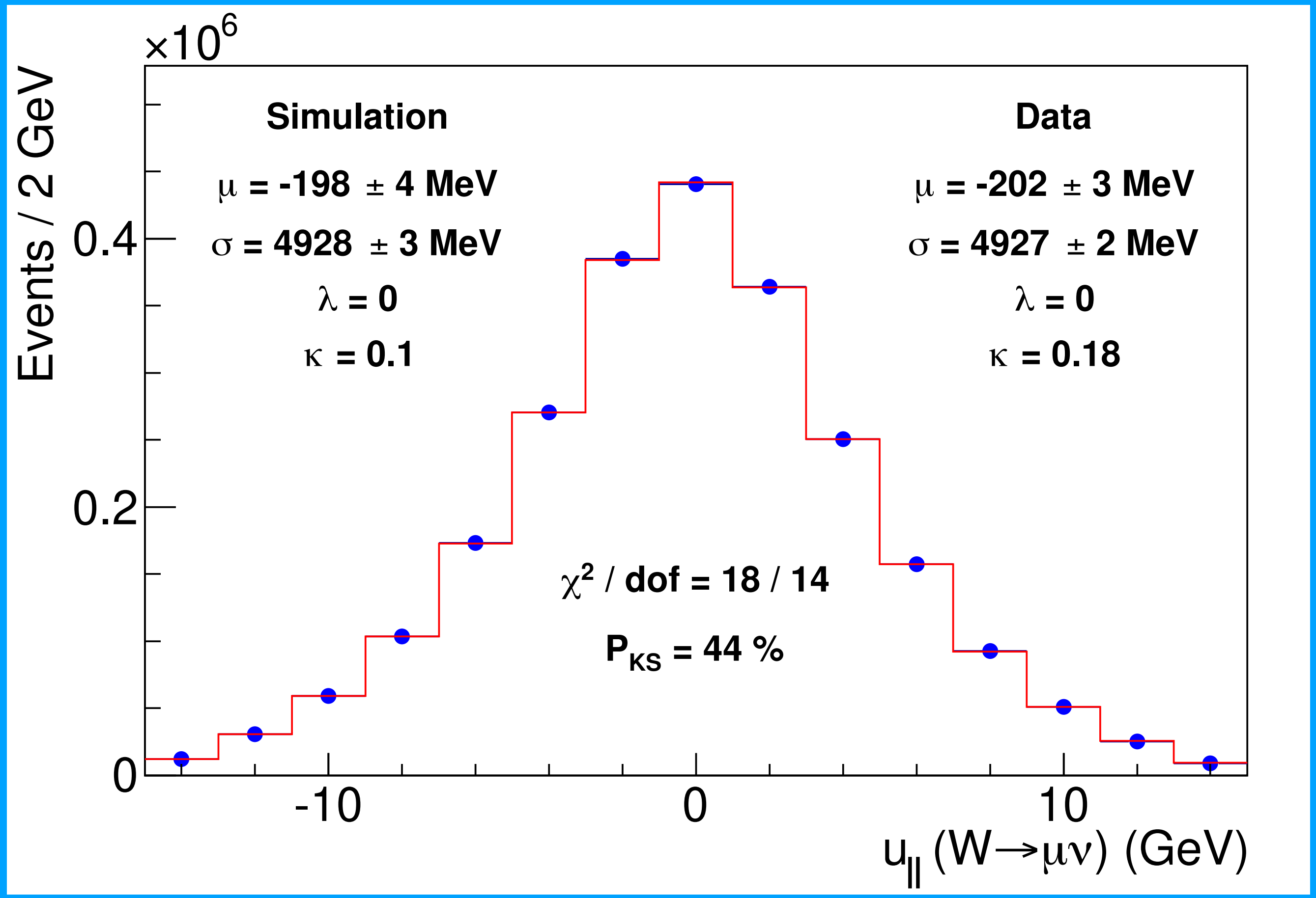

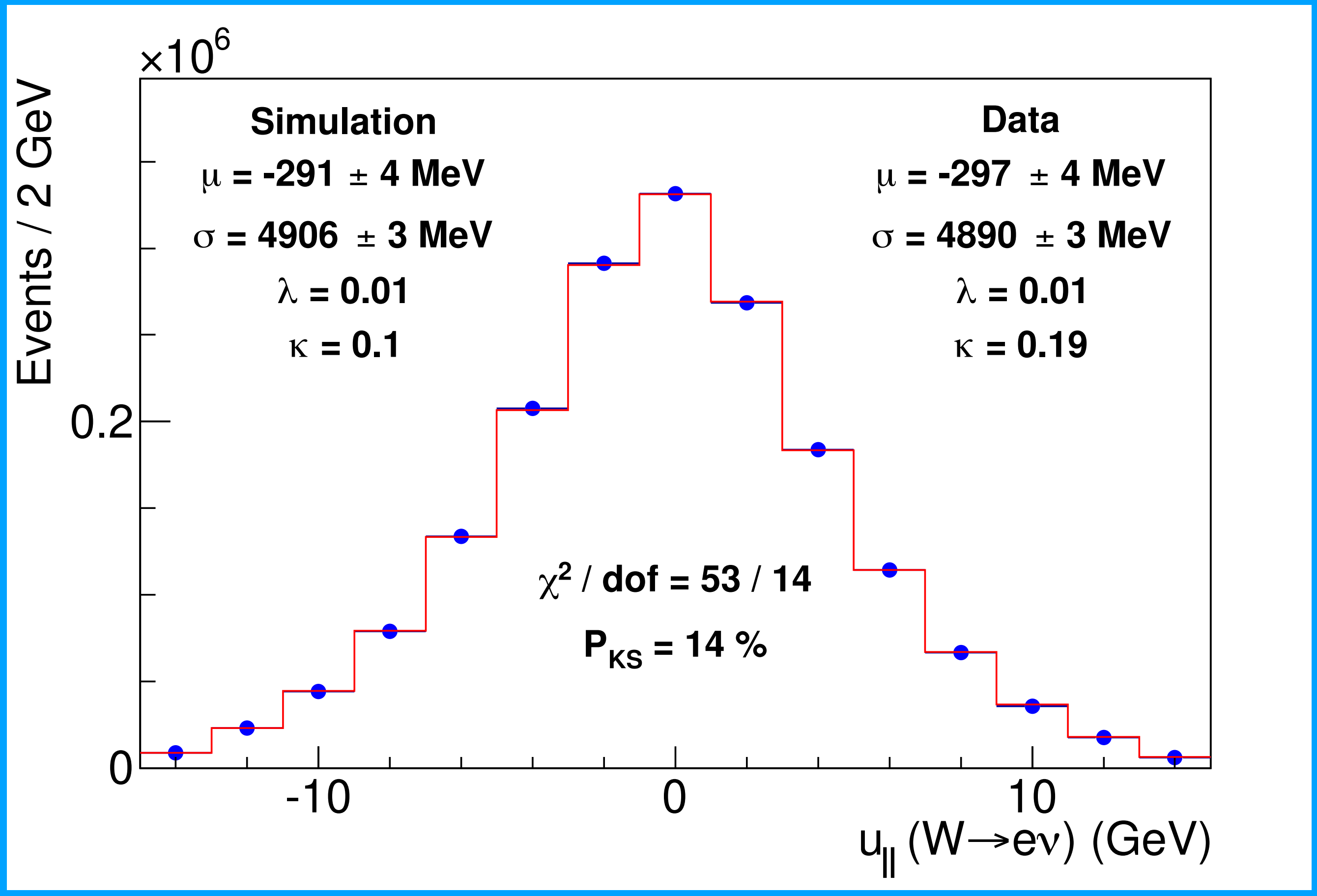

W boson production

Transverse mass insensitive to p_T^W to first order

O(1 MeV) change in m_W for each % change in p_T^W from 0-30 GeV

Lepton p_T distributions more sensitive to p_T^W

Generate events with Resbos: non-perturbative parameters & NNLL resummation

Z boson p_T constrains non-perturbative parameter(s)

Determine $p_T^Z \to p_T^W$ uncertainty using DYQT perturbative & resummation scale variations

Use observed W recoil spectrum to constrain scale variations

Similar uncertainty between correlating W & Z scales and not correlating them

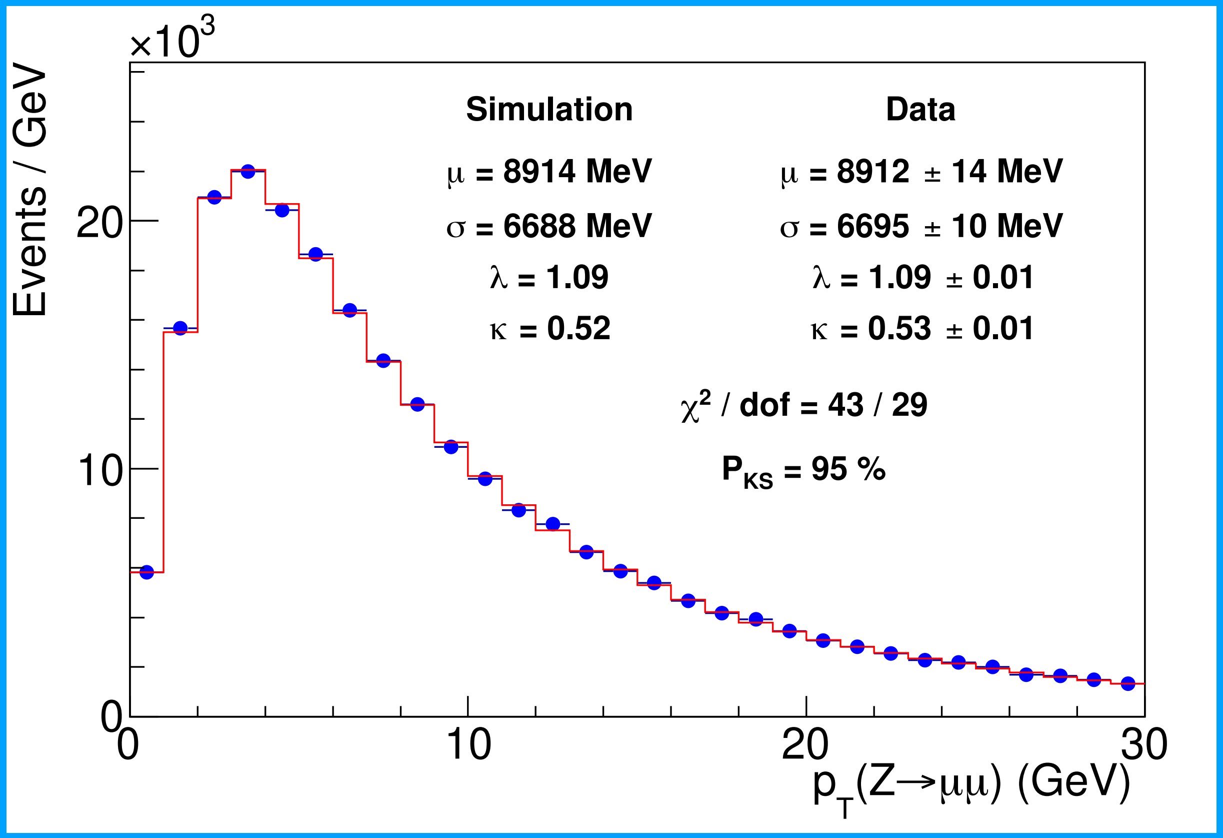

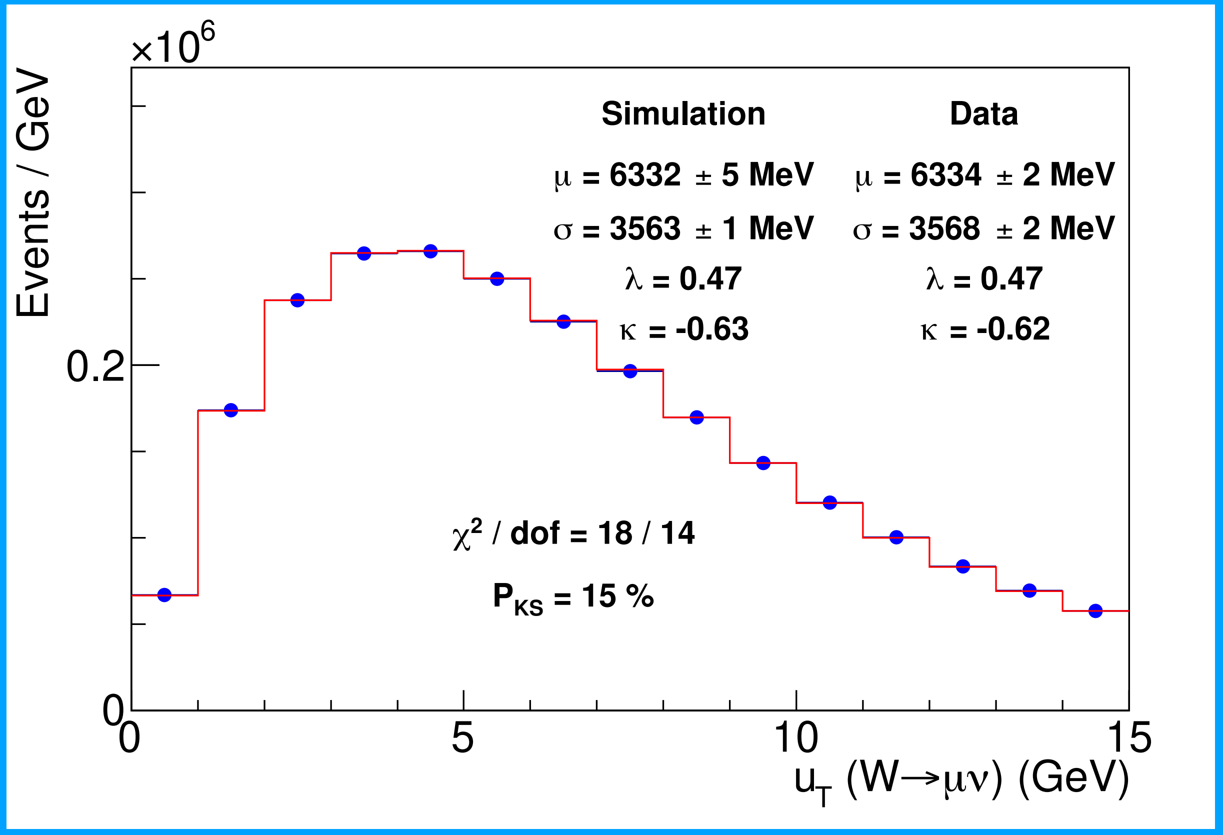

W boson candidates

W boson event selection
require kinematics consistent with resonance production

2.4 M $W \to \mu\nu$ candidates
1.8 M $W \to e\nu$ candidates

Lepton identification
No lepton isolation requirement in trigger or offline selection
High efficiency with little recoil dependence

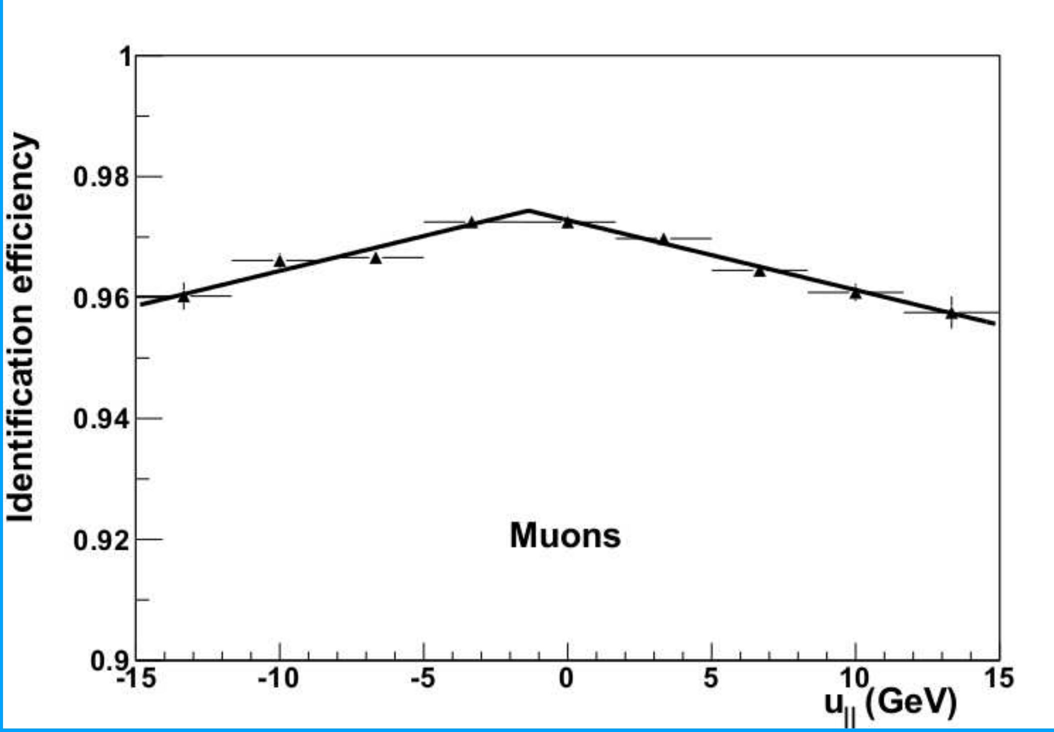

Backgrounds
Most challenging background comes from hadrons misreconstructed as leptons (0.2-0.3%)

W boson mass measurement

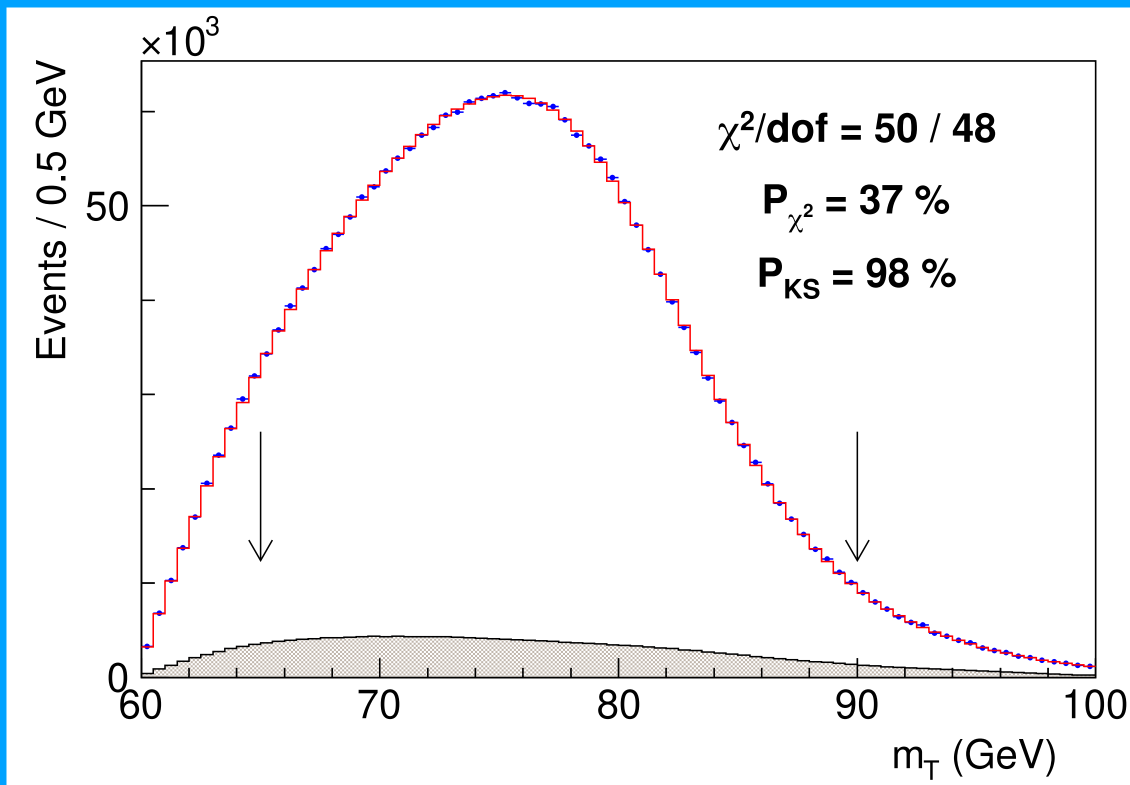

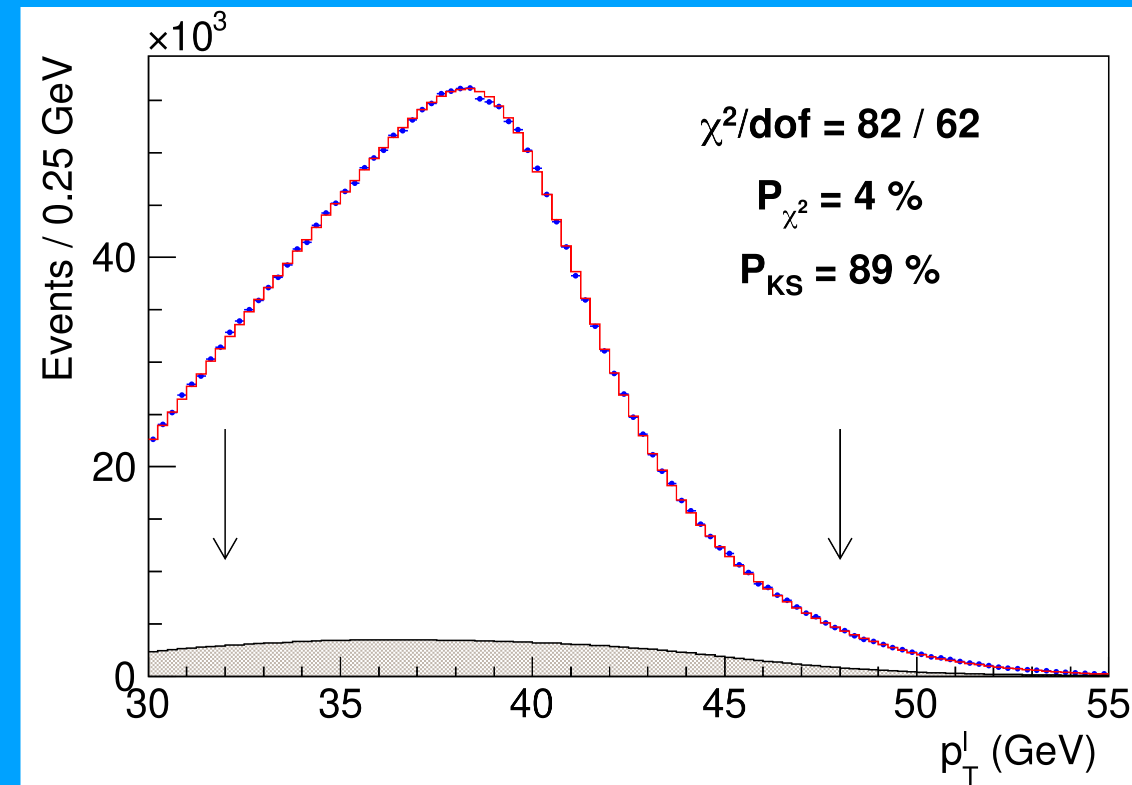

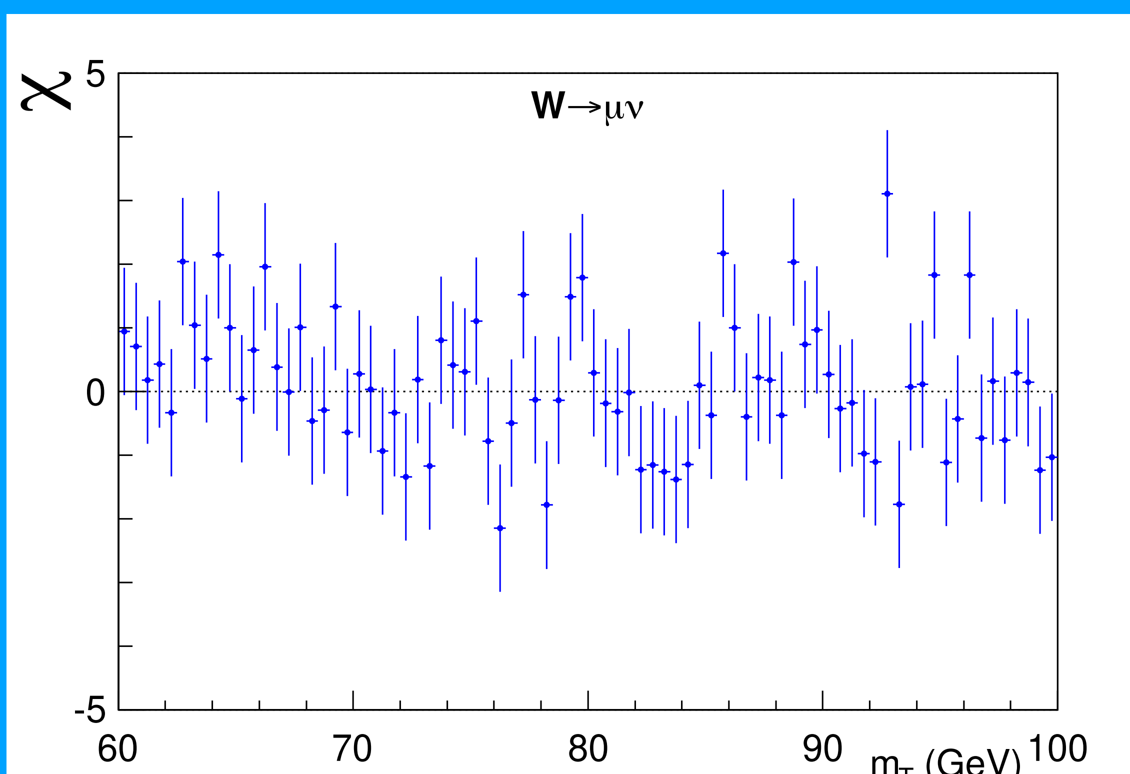

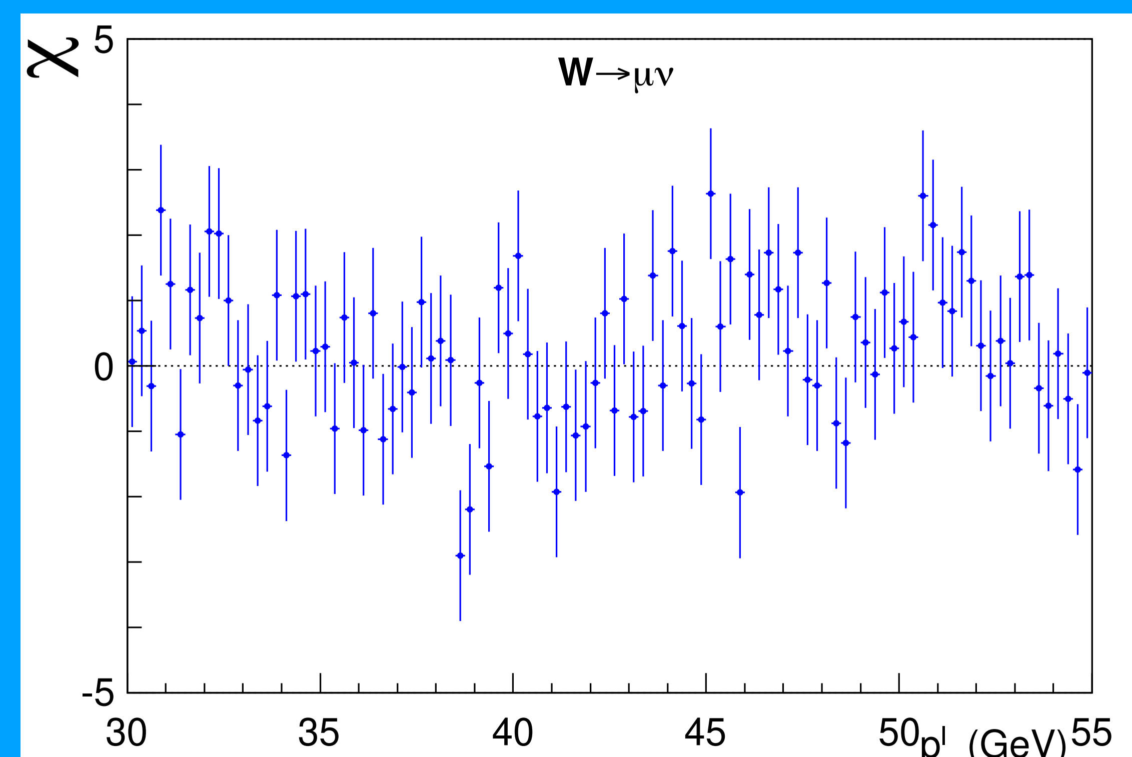

W boson mass measurement

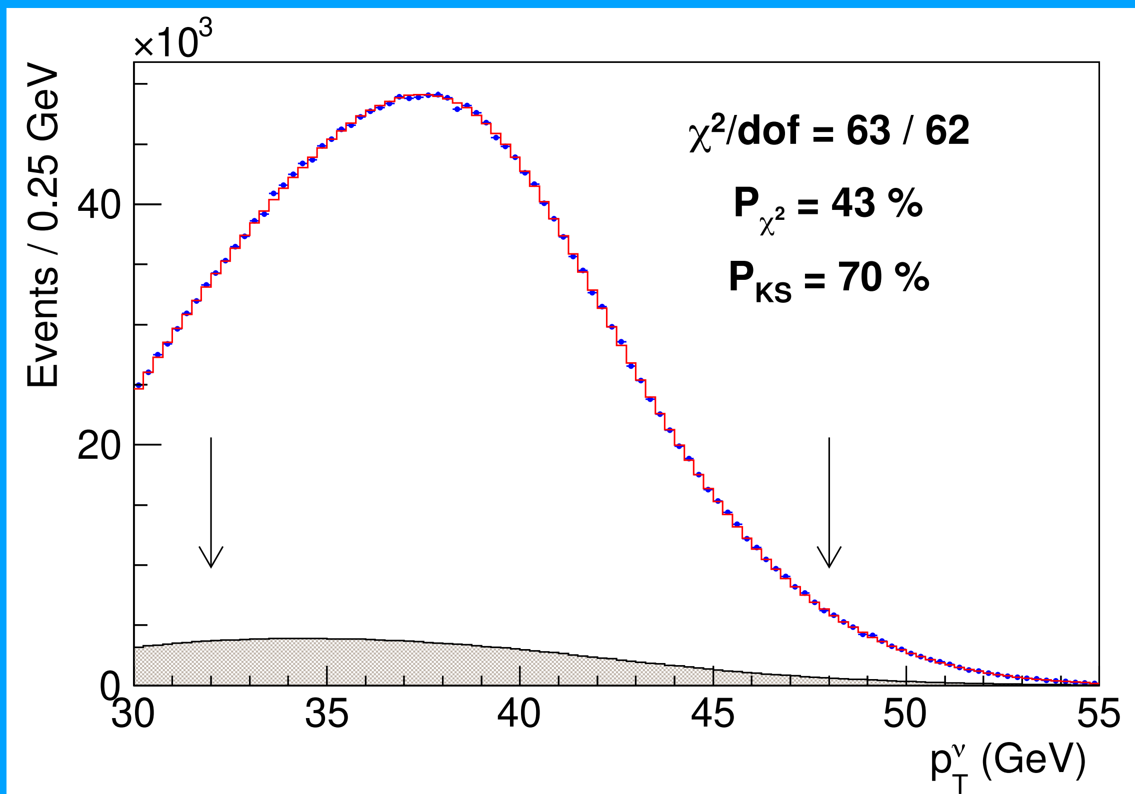

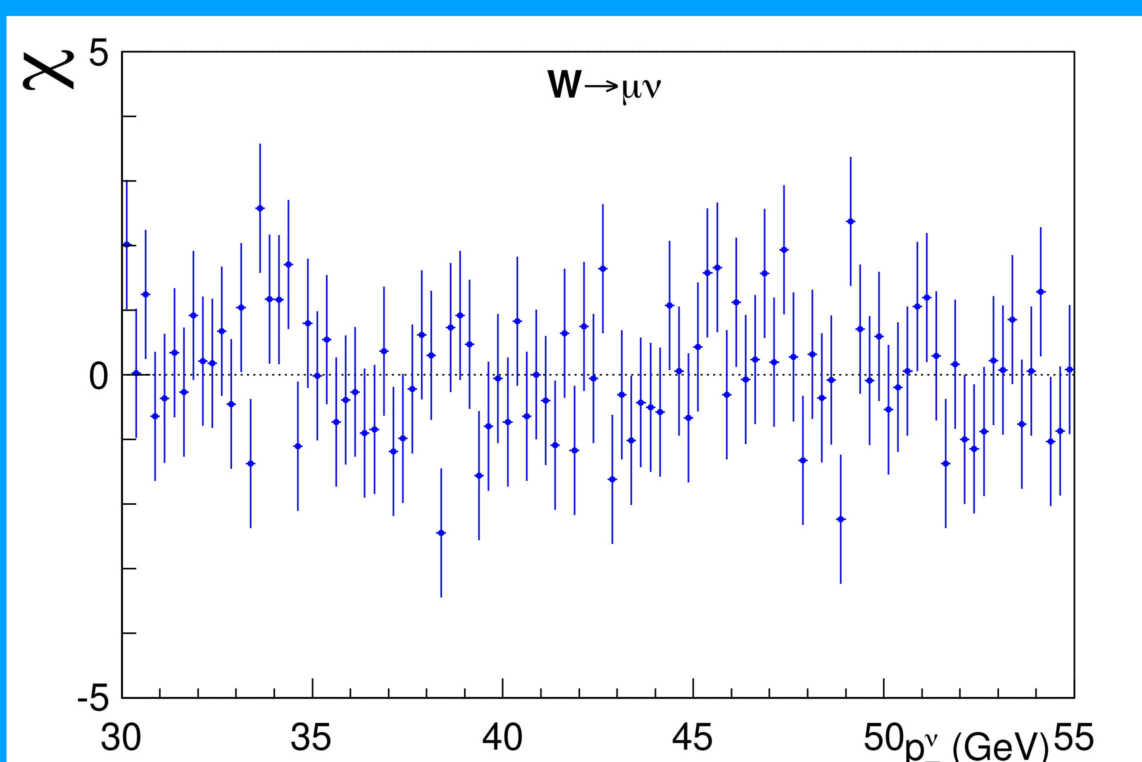

Distribution	W-boson mass (MeV)	χ^2/dof
$m_T(e,\nu)$	$80\ 429.1 \pm 10.3_{\text{stat}} \pm 8.5_{\text{syst}}$	39/48
$p_T^{\ell}(e)$	$80\ 411.4 \pm 10.7_{\text{stat}} \pm 11.8_{\text{syst}}$	83/62
$p_T^{\nu}(e)$	$80\ 426.3 \pm 14.5_{\text{stat}} \pm 11.7_{\text{syst}}$	69/62
$m_T(\mu,\nu)$	$80\ 446.1 \pm 9.2_{\text{stat}} \pm 7.3_{\text{syst}}$	50/48
$p_T^{\ell}(\mu)$	$80\ 428.2 \pm 9.6_{\text{stat}} \pm 10.3_{\text{syst}}$	82/62
$p_T^{\nu}(\mu)$	$80\ 428.9 \pm 13.1_{\text{stat}} \pm 10.9_{\text{syst}}$	63/62
combination	$80\ 433.5 \pm 6.4_{\text{stat}} \pm 6.9_{\text{syst}}$	7.4/5

W boson mass measurement

Combination	m_T fit		p_T^ℓ fit		p_T^ν fit		Value (MeV)	χ^2/dof	Probability (%)
	Electrons	Muons	Electrons	Muons	Electrons	Muons			
m_T	✓	✓					$80\,439.0 \pm 9.8$	1.2 / 1	28
p_T^ℓ			✓	✓			$80\,421.2 \pm 11.9$	0.9 / 1	36
p_T^ν					✓	✓	$80\,427.7 \pm 13.8$	0.0 / 1	91
Electrons	✓		✓		✓		$80\,424.6 \pm 13.2$	3.3 / 2	19
Muons		✓		✓		✓	$80\,437.9 \pm 11.0$	3.6 / 2	17
All	✓	✓	✓	✓	✓	✓	$80\,433.5 \pm 9.4$	7.4 / 5	20

Fit difference	Muon channel	Electron channel
$M_W(\ell^+) - M_W(\ell^-)$	$-7.8 \pm 18.5_{\text{stat}} \pm 12.7_{\text{COT}}$	$14.7 \pm 21.3_{\text{stat}} \pm 7.7_{\text{stat}}^{\text{E/p}}$ $(0.4 \pm 21.3_{\text{stat}})$
$M_W(\phi_\ell > 0) - M_W(\phi_\ell < 0)$	$24.4 \pm 18.5_{\text{stat}}$	$9.9 \pm 21.3_{\text{stat}} \pm 7.5_{\text{stat}}^{\text{E/p}}$ $(-0.8 \pm 21.3_{\text{stat}})$
$M_Z(\text{run} > 271100) - M_Z(\text{run} < 271100)$	$5.2 \pm 12.2_{\text{stat}}$	$63.2 \pm 29.9_{\text{stat}} \pm 8.2_{\text{stat}}^{\text{E/p}}$ $(-16.0 \pm 29.9_{\text{stat}})$

W boson mass measurements

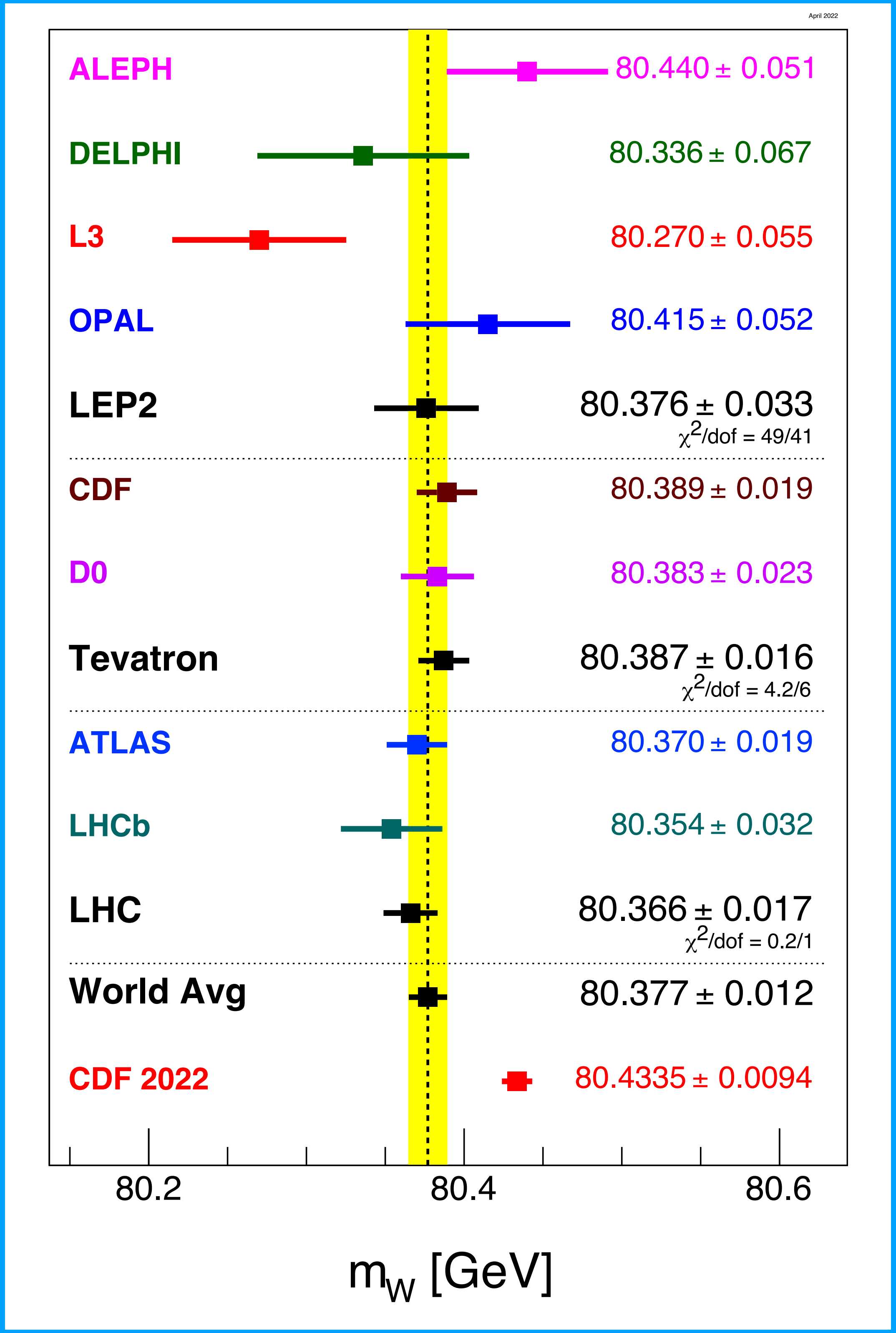

Summary

The W boson mass is a sensitive quantity to high-scale physics

Measurement with <10 MeV precision (~0.01%) achieved using the complete CDF data set

Result of >20 years of experience with the CDF II detector

Surprising 0.1% deviation from SM motivates expanded study of m_W measurements and procedures

Backup

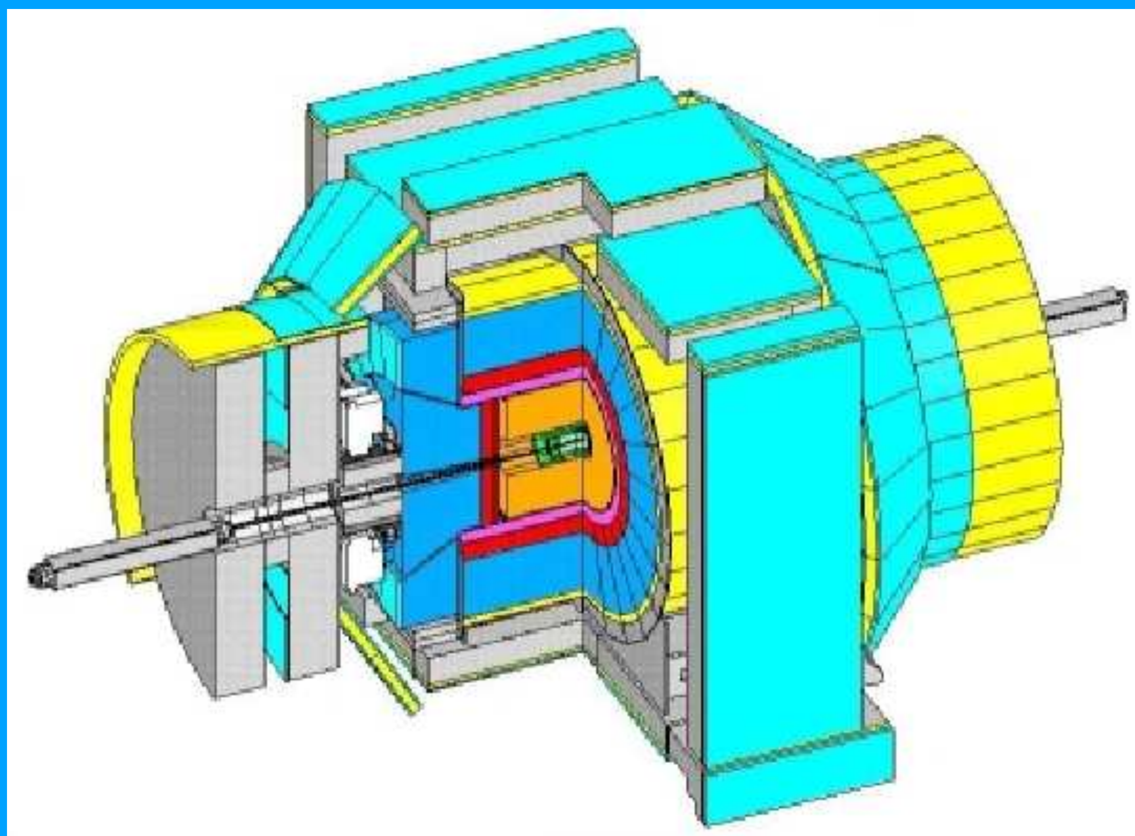

2.2/fb result

Distribution	M_W (MeV)	χ^2/d.o.f.
$W \to e\nu$		
m_T	80408 ± 19	52/48
p_T^ℓ	80393 ± 21	60/62
p_T^ν	80431 ± 25	71/62
$W \to \mu\nu$		
m_T	80379 ± 16	57/48
p_T^ℓ	80348 ± 18	58/62
p_T^ν	80406 ± 22	82/62

background fractions

Source	Fraction (%)	δM_W (MeV) m_T fit	p_T^μ fit	p_T^ν fit
$Z/\gamma^* \to \mu\mu$	7.37 ± 0.10	1.6 (0.7)	3.6 (0.3)	0.1 (1.5)
$W \to \tau\nu$	0.880 ± 0.004	0.1 (0.0)	0.1 (0.0)	0.1 (0.0)
Hadronic jets	0.01 ± 0.04	0.1 (0.8)	-0.6 (0.8)	2.4 (0.5)
Decays in flight	0.20 ± 0.14	1.3 (3.1)	1.3 (5.0)	-5.2 (3.2)
Cosmic rays	0.01 ± 0.01	0.3 (0.0)	0.5 (0.0)	0.3 (0.3)
Total	8.47 ± 0.18	2.1 (3.3)	3.9 (5.1)	5.7 (3.6)

Source	Fraction (%)	δM_W (MeV) m_T fit	p_T^e fit	p_T^ν fit
$Z/\gamma^* \to ee$	0.134 ± 0.003	0.2 (0.3)	0.3 (0.0)	0.0 (0.6)
$W \to \tau\nu$	0.94 ± 0.01	0.6 (0.0)	0.6 (0.0)	0.6 (0.0)
Hadronic jets	0.34 ± 0.08	2.2 (1.2)	0.9 (6.5)	6.2 (-1.1)
Total	1.41 ± 0.08	2.3 (1.2)	1.1 (6.5)	6.2 (1.3)

W boson production and decay

Parton distributions impact the measurement through lepton acceptance

Restriction in η reduces the fraction of low-p_T leptons

Small correction applied to update to NNPDF3.1 NNLO PDF

The set with the most W charge asymmetry measurements at the time

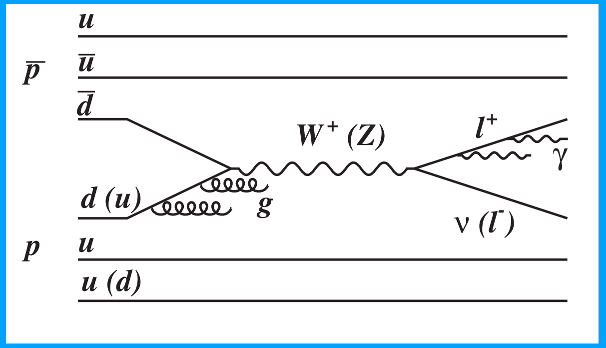

Uncertainty determined using a principal component analysis on the replica set

Measurement sensitive to ~15 eigenvectors

Leading 25 eigenvectors used to estimate uncertainty (3.9 MeV)

Three general NNLO PDF sets (NNPDF3.1, CT18, and MMHT14) have a range of ± 2.1 MeV from mean

W^+ initial	Type	Pythia LO	Madgraph LO	Madgraph NLO
u dbar	v-v	81.7%	82.0%	82.7%
dbar u	s-s	8.9%	9.0%	8.8%
u sbar	v-s	1.6%	1.9%	1.8%
sbar u	s-s	0.3%	0.3%	0.3%
c sbar	s-s	2.9%	2.9%	-
sbar c	s-s	2.9%	2.9%	-
c dbar	s-v	0.7%	0.7%	-
dbar c	s-s	0.2%	0.2%	-
u g	v-g		-	3.7%
g dbar	g-v		-	1.8%
g u	g-s		-	0.4%
dbar g	s-g		-	0.5%
g sbar	g-s		-	0.02%
sbar g	s-g		-	0.02%

Photos resummation with ME corrections used to model final-state photon radiation

validated by studying the average radiation in EM towers around the charged lepton, and with the Z mass measurement

Combination and compatibility of m_W measurements

Working group to combining the measurements from CDF, D0, ATLAS, LHCb, and the LEP experiments

Update measurements to a common PDF set and a common calculation of W boson polarization

Simulate events with custom fast simulations

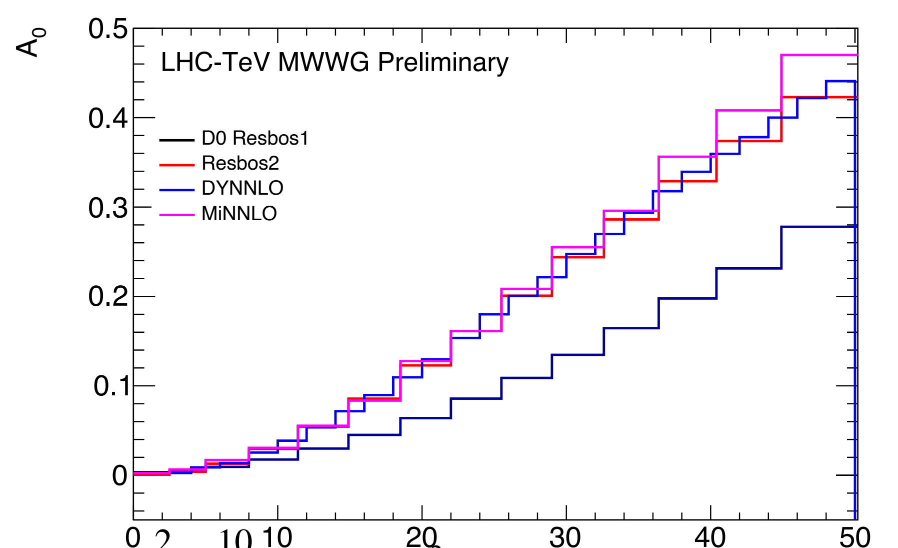

$$A_0 = \frac{2}{3} + \frac{10}{3} < 1 - 3\cos^2\theta >$$

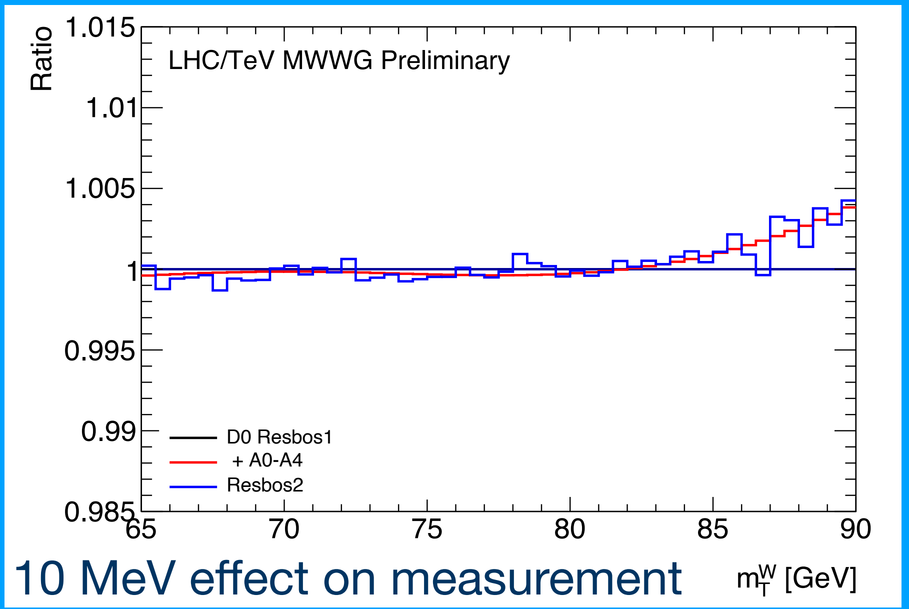

10 MeV effect on measurement

$$w_{A_i \to A'_i}(\cos\theta, \phi; p_T^W, y_W) = \frac{(1+\cos^2\theta) + \sum_i A'_i(p_T^W, y_W) f_i(\theta;\phi)}{(1+\cos^2\theta) + \sum_i A_i(p_T^W, y_W) f_i(\theta;\phi)},$$

Dataset	NNPDF31	NNPDF40	MMHT14	MSHT20	CT18NNLO	ABMP16
CDF Z rapidity	24|28 / 28	28|30 / 28	30|31 / 28	32|32 / 28	27|27 / 28	31|31 / 28
CDF W asymmetry	11|57 / 13	14|17 / 13	12|13 / 13	28|27 / 13	11|35 / 13	21|43 / 13
D0 Z rapidity	22|22 / 28	23|23 / 28	23|23 / 28	24|23 / 28	22|22 / 28	22|22 / 28
D0 $We\nu$ lepton asymmetry	22|32 / 13	23|29 / 13	52|51 / 13	42|40 / 13	19|32 / 13	26|24 / 13
D0 $W\mu\nu$ lepton asymmetry	12|14 / 10	12|16 / 10	11|14 / 10	11|13 / 10	12|13 / 10	11|12 / 10
ATLAS peak CC Z rapidity	13|18 / 12	13|17 / 12	58|89 / 12	17|19 / 12	11|77 / 12	18|32 / 12
ATLAS W^- lepton rapidity	12|18 / 11	12|15 / 11	33|33 / 11	16|17 / 11	9.9|28 / 11	14|17 / 11
ATLAS W^+ lepton rapidity	8.9|13 / 11	8.6|11 / 11	15|21 / 11	12|13 / 11	9.4|16 / 11	10|12 / 11
Correlated χ^2	76|110	63|83	212|236	91|102	43|251	86|108
Log penalty χ^2	-0.62|-0.62	-0.58|-0.58	-1.62|-1.62	-2.89|-2.89	-1.68|-1.68	-2.72|-2.72
Total χ^2 / dof	200|312 / 126	195|242 / 126	445|509 / 126	270|283 / 126	163|499 / 126	236|300 / 126
χ^2 p-value	0.00	0.00	0.00	0.00	0.02	0.00

Measurement updates

updates relative to 2.2/fb result

Method or technique	impact
Detailed treatment of parton distribution functions	+3.5 MeV
Resolved beam-constraining bias in CDF reconstruction	+10 MeV
Improved COT alignment and drift model [65]	uniformity
Improved modeling of calorimeter tower resolution	uniformity
Temporal uniformity calibration of CEM towers	uniformity
Lepton removal procedure corrected for luminosity	uniformity
Higher-order calculation of QED radiation in J/ψ and Υ decays	accuracy
Modeling kurtosis of hadronic recoil energy resolution	accuracy
Improved modeling of hadronic recoil angular resolution	accuracy
Modeling dijet contribution to recoil resolution	accuracy
Explicit luminosity matching of pileup	accuracy
Modeling kurtosis of pileup resolution	accuracy
Theory model of p_T^W/p_T^Z spectrum ratio	accuracy
Constraint from p_T^W data spectrum	robustness
Cross-check of p_T^Z tuning	robustness

Future possibilities

Recoil tuning
- Fine-tune calorimeter response corrections in data
- Calibrate a shower Monte Carlo

Recoil validation
- Compare W & Z response in events with a single lepton (remove any additional lepton)
- Compare W & Z energy flows

Event generation
- Generate events using a higher-order calculation
- Validate p_T^W using high/low p_T^l asymmetry
- Validate PDF using low $p_T l$ region and rapidity-dependent mass fits

Event selection
- Vary lepton id (add isolation)

Analysis updates
- Identify the effect of each analysis change in the muon channel

Luminosity & time dependence
- Fit mass in subsets in time or luminosity

Uncertainties

Source	Uncertainty (MeV)
Lepton energy scale	3.0
Lepton energy resolution	1.2
Recoil energy scale	1.2
Recoil energy resolution	1.8
Lepton efficiency	0.4
Lepton removal	1.2
Backgrounds	3.3
p_T^Z model	1.8
p_T^W/p_T^Z model	1.3
Parton distributions	3.9
QED radiation	2.7
W boson statistics	6.4
Total	9.4

Source of systematic	m_T fit			p_T^ℓ fit			p_T^ν fit		
uncertainty	Electrons	Muons	Common	Electrons	Muons	Common	Electrons	Muons	Common
Lepton energy scale	5.8	2.1	1.8	5.8	2.1	1.8	5.8	2.1	1.8
Lepton energy resolution	0.9	0.3	-0.3	0.9	0.3	-0.3	0.9	0.3	-0.3
Recoil energy scale	1.8	1.8	1.8	3.5	3.5	3.5	0.7	0.7	0.7
Recoil energy resolution	1.8	1.8	1.8	3.6	3.6	3.6	5.2	5.2	5.2
Lepton $u_{\|\|}$ efficiency	0.5	0.5	0	1.3	1.0	0	2.6	2.1	0
Lepton removal	1.0	1.7	0	0	0	0	2.0	3.4	0
Backgrounds	2.6	3.9	0	6.6	6.4	0	6.4	6.8	0
p_T^Z model	0.7	0.7	0.7	2.3	2.3	2.3	0.9	0.9	0.9
p_T^W/p_T^Z model	0.8	0.8	0.8	2.3	2.3	2.3	0.9	0.9	0.9
Parton distributions	3.9	3.9	3.9	3.9	3.9	3.9	3.9	3.9	3.9
QED radiation	2.7	2.7	2.7	2.7	2.7	2.7	2.7	2.7	2.7
Statistical	10.3	9.2	0	10.7	9.6	0	14.5	13.1	0
Total	13.5	11.8	5.8	16.0	14.1	7.9	18.8	17.1	7.4

Electron momentum calibration

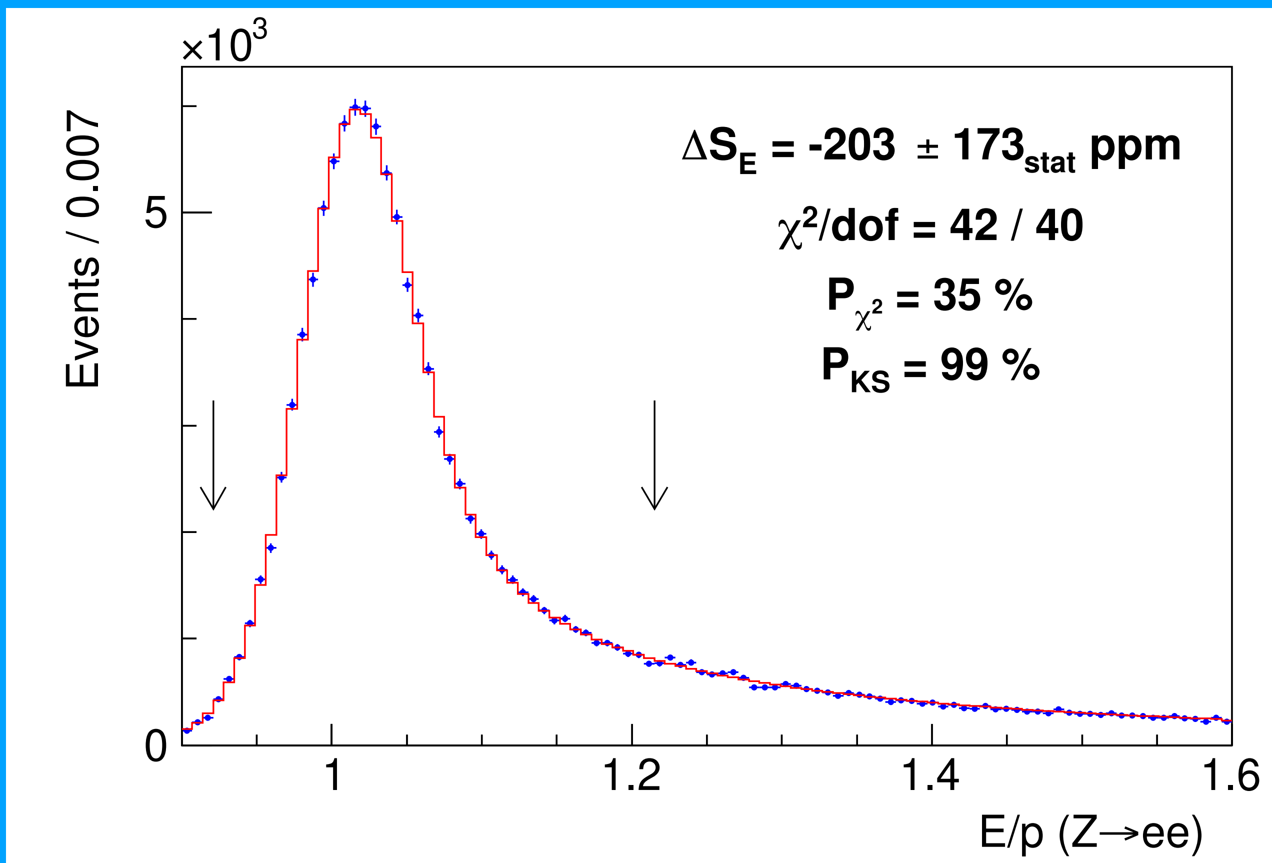

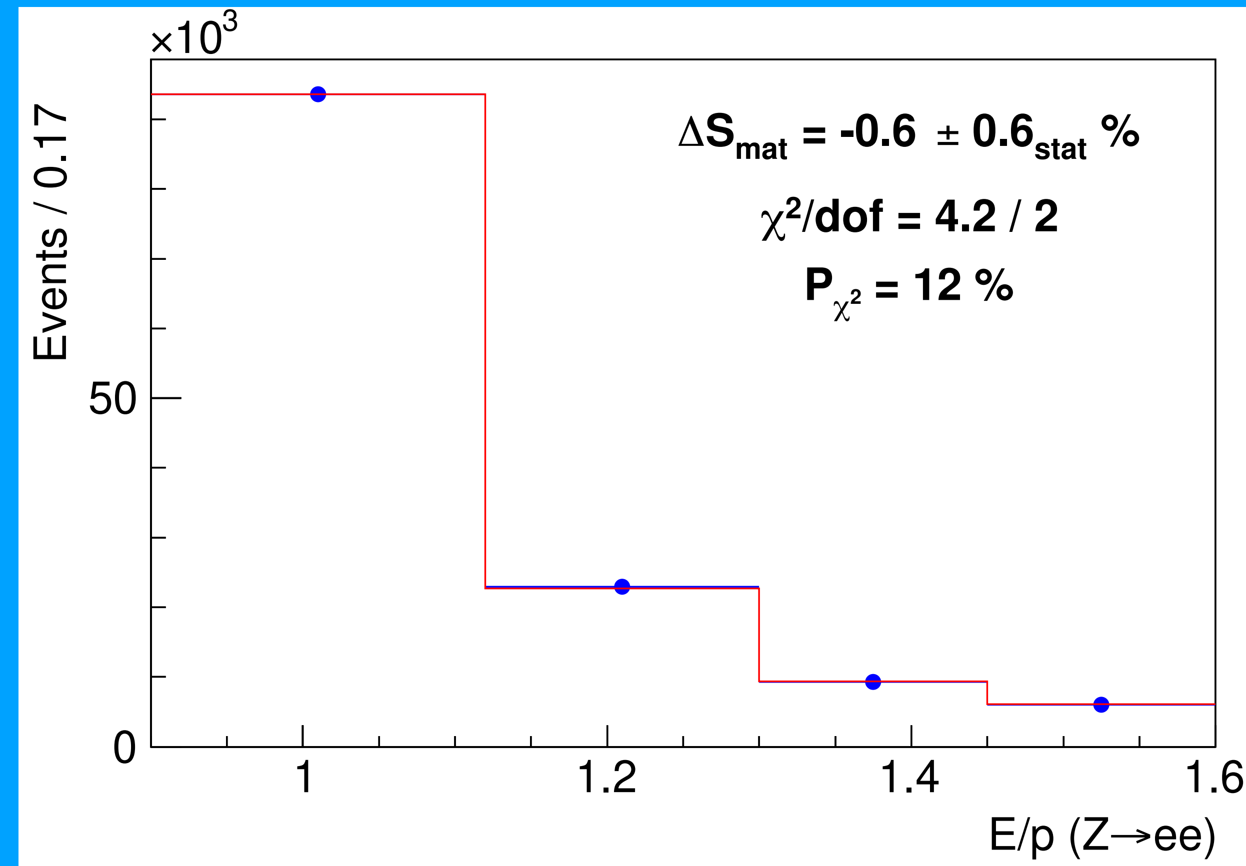

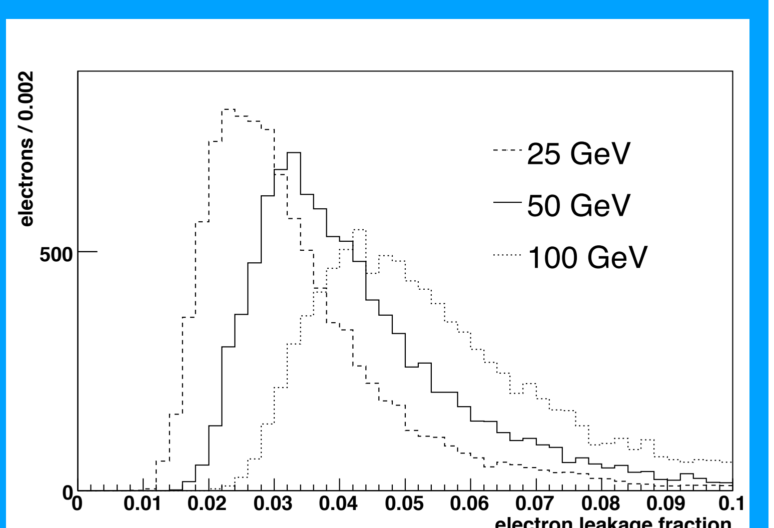

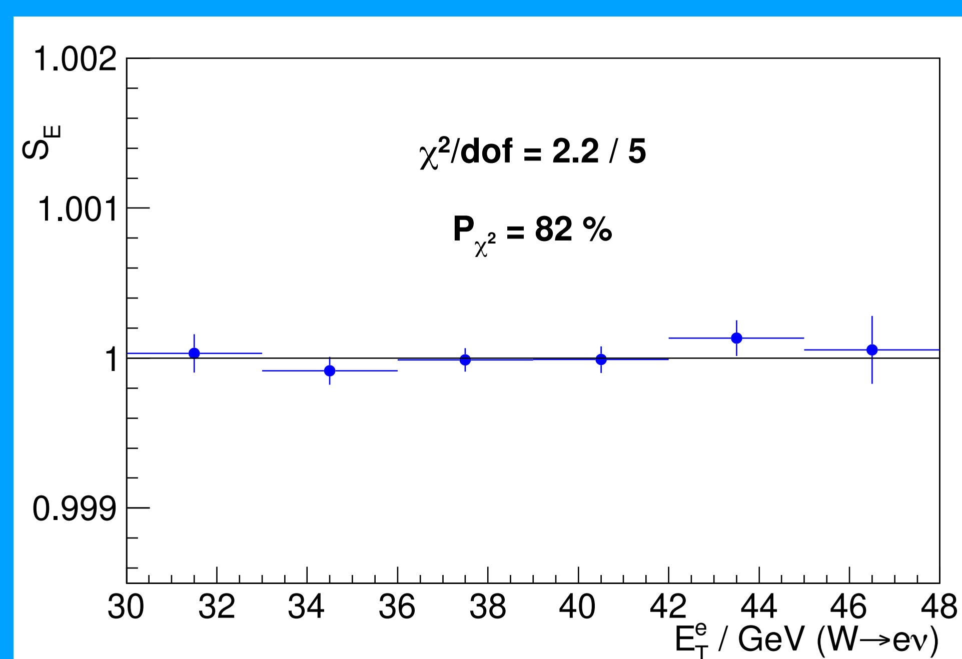

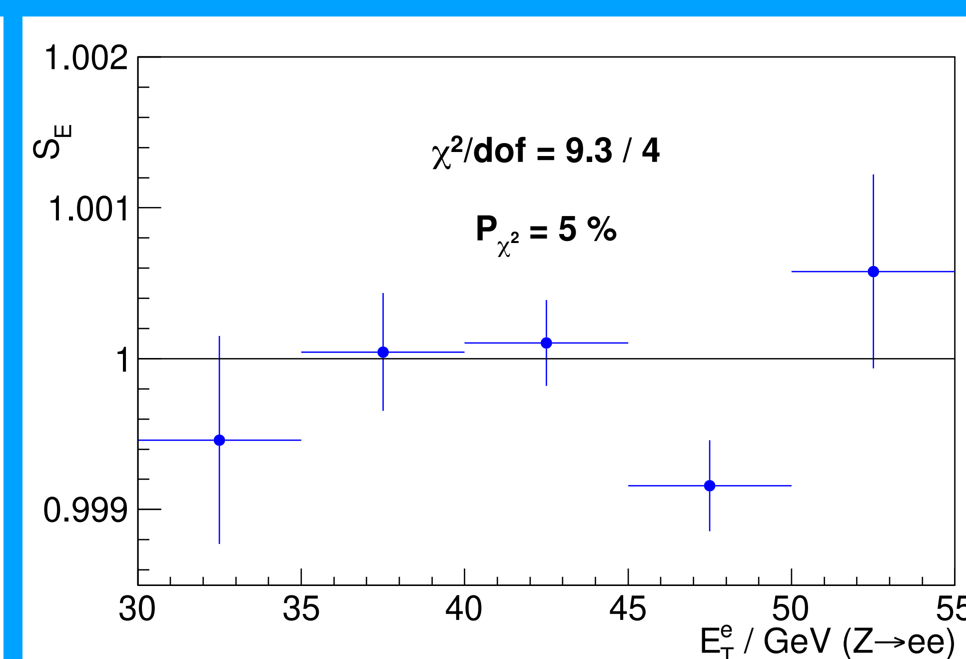

Recoil in W & Z events

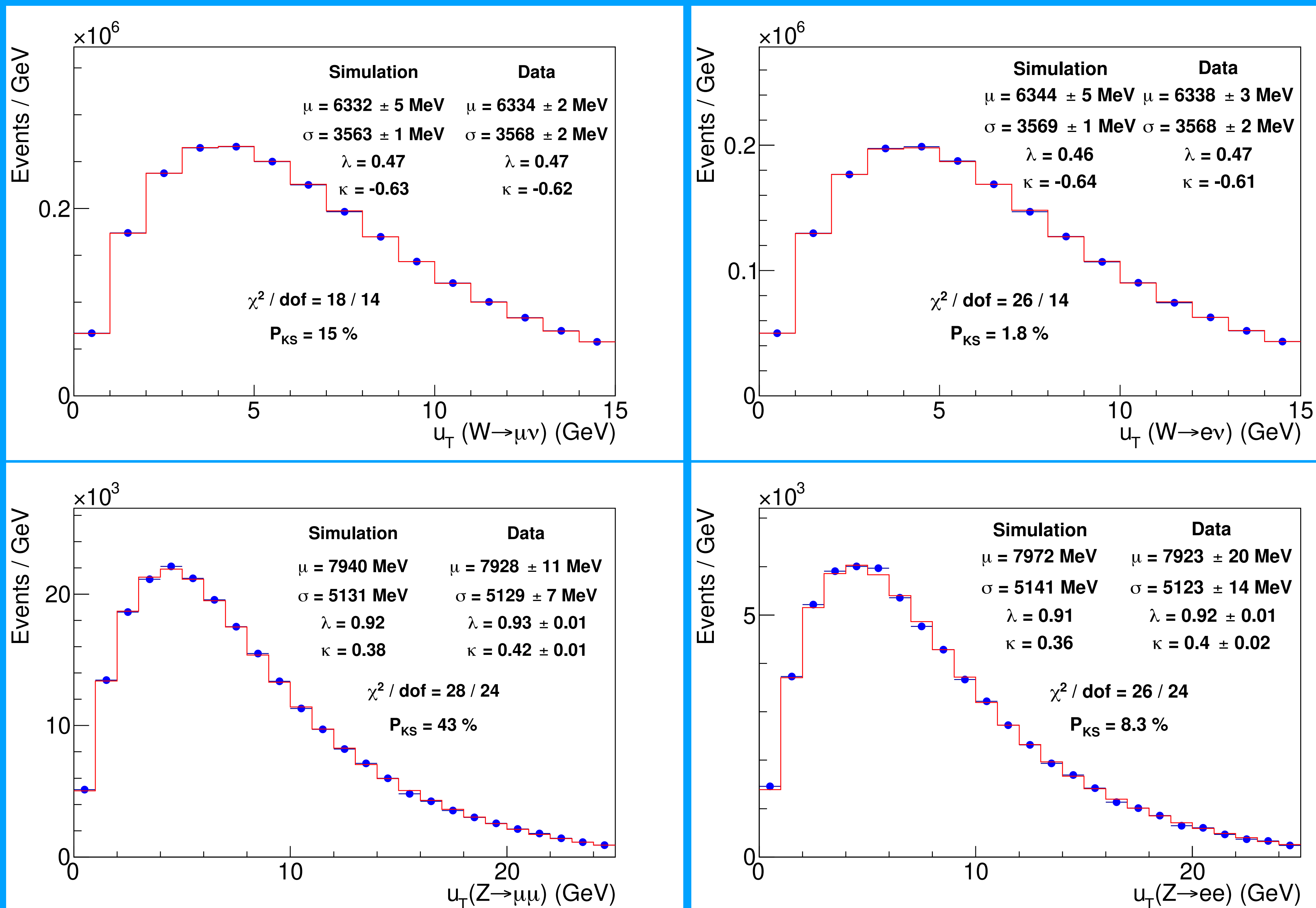

Recoil projections in W events

Parameter	Description	Source	m_T	p_T^ℓ	p_T^ν
a	average response	Fig. S23	−1.6	−2.9	−0.2
b	response non-linearity	Fig. S23	−0.8	−2.0	0.7
Response			1.8	3.5	0.7
N_V	spectator interactions	Fig. S24	0.5	−3.2	3.6
s_{had}	sampling resolution	Fig. S24	0.3	0.3	0.8
$f_{\pi^0}^4$	EM fluctuations at low u_T	Fig. S25	−0.3	−0.2	−1.0
$f_{\pi^0}^{15}$	EM fluctuations at high u_T	Fig. S25	−0.3	−0.3	−0.2
α	angular resolution at low u_T	Fig. S26	1.4	0.1	2.5
β	angular resolution at intermediate u_T	Fig. S26	0.2	0.1	0.7
γ	angular resolution at high u_T	Fig. S26	0.3	0.3	0.7
f_2^a	average dijet component	Fig. S27	0.1	−1.1	0.8
f_2^s	variation of dijet component with u_T	Fig. S27	−0.1	−0.2	−0.1
k_ξ	average dijet resolution	Fig. S28	−0.1	0.1	−0.3
δ_ξ	fluctuations in dijet resolution	Fig. S28	−0.2	0.2	−1.1
A_ξ	higher-order term in dijet resolution	Fig. S28	0.1	−1.0	0.7
μ_ξ	—"—	Fig. S28	−0.5	−0.4	−0.9
ϵ_ξ	—"—	Fig. S28	0.1	−0.2	0.4
S_ξ^+	—"—	Fig. S28	0.5	−0.4	1.4
S_ξ^-	—"—	Fig. S28	−0.3	−0.2	−0.5
q_ξ	—"—	Fig. S28	−0.2	0.0	0.2
Resolution			1.8	3.6	5.2

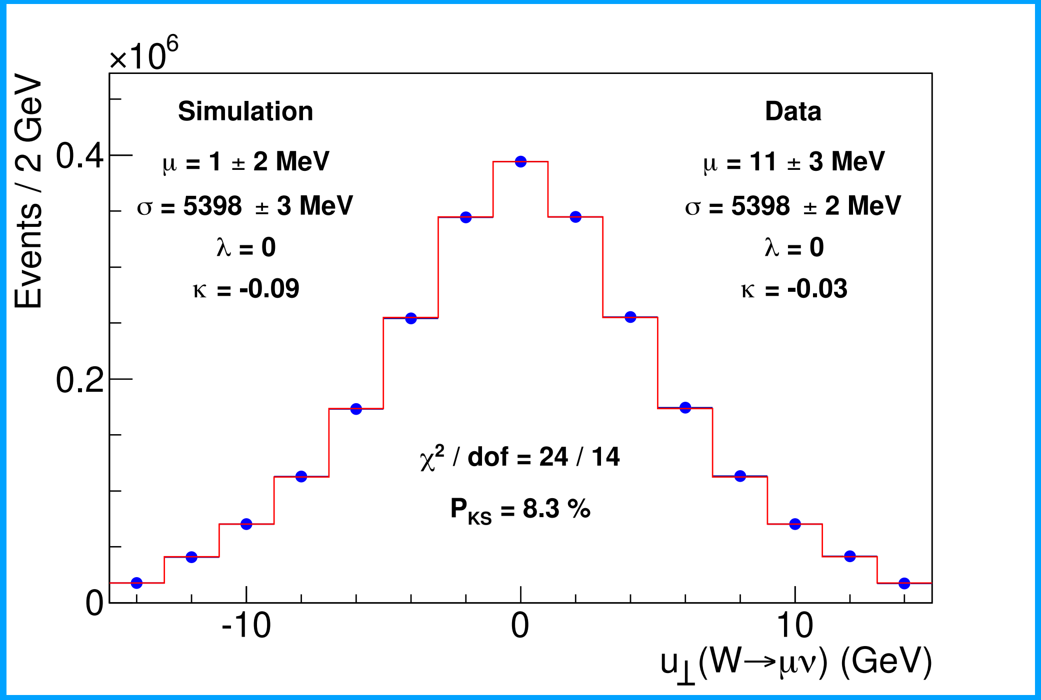

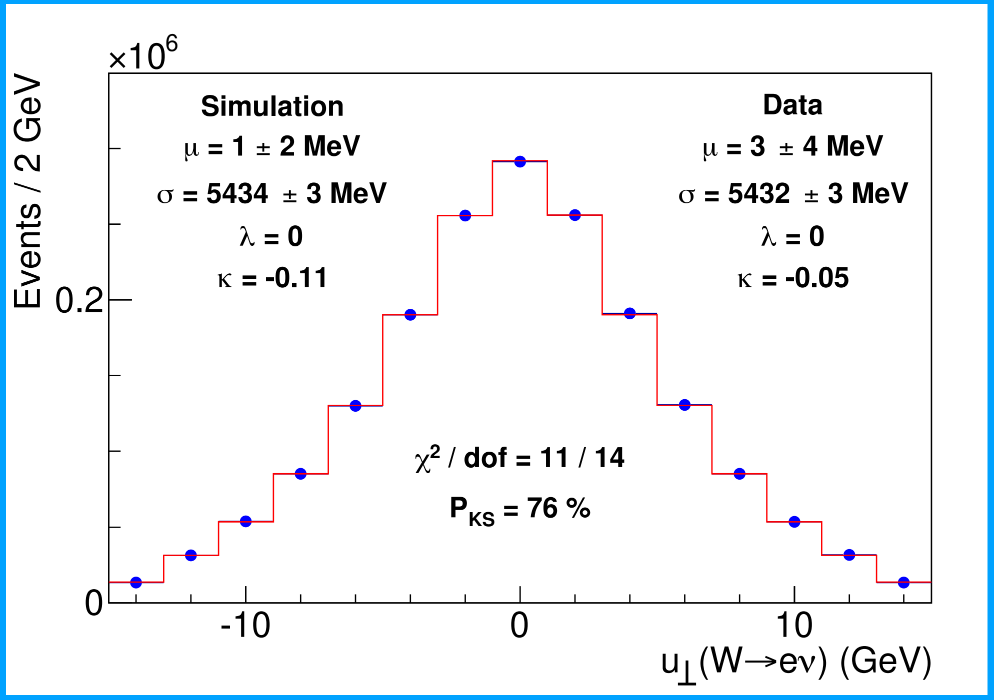

Recoil reconstruction in muon channel

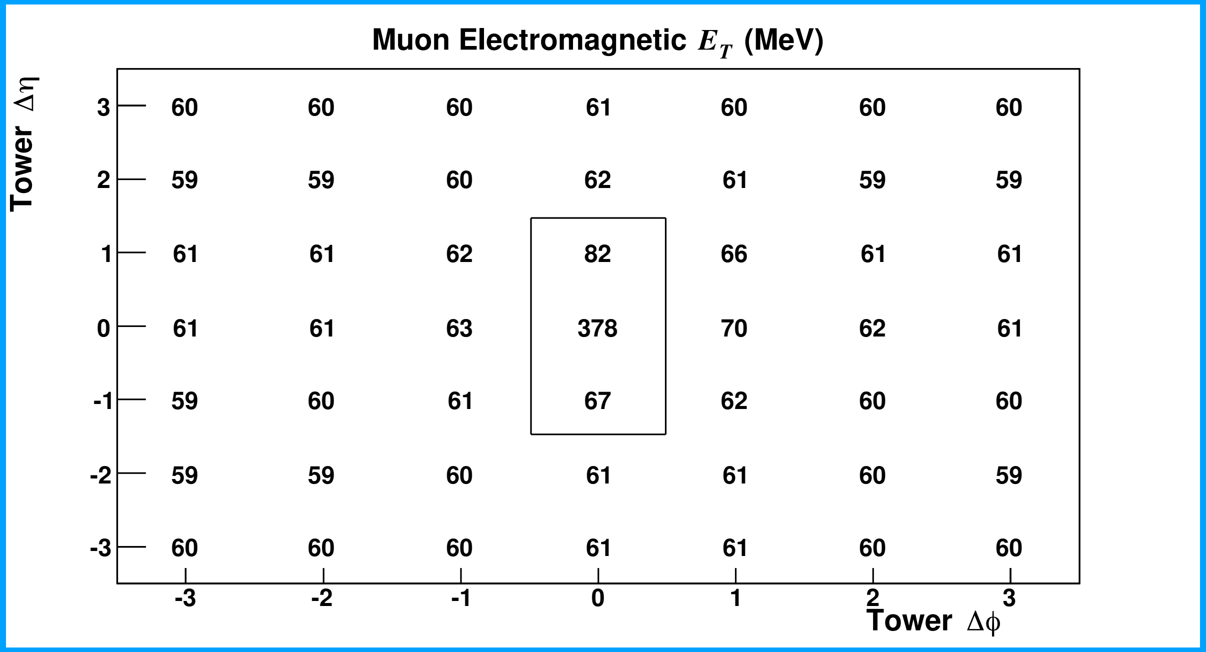

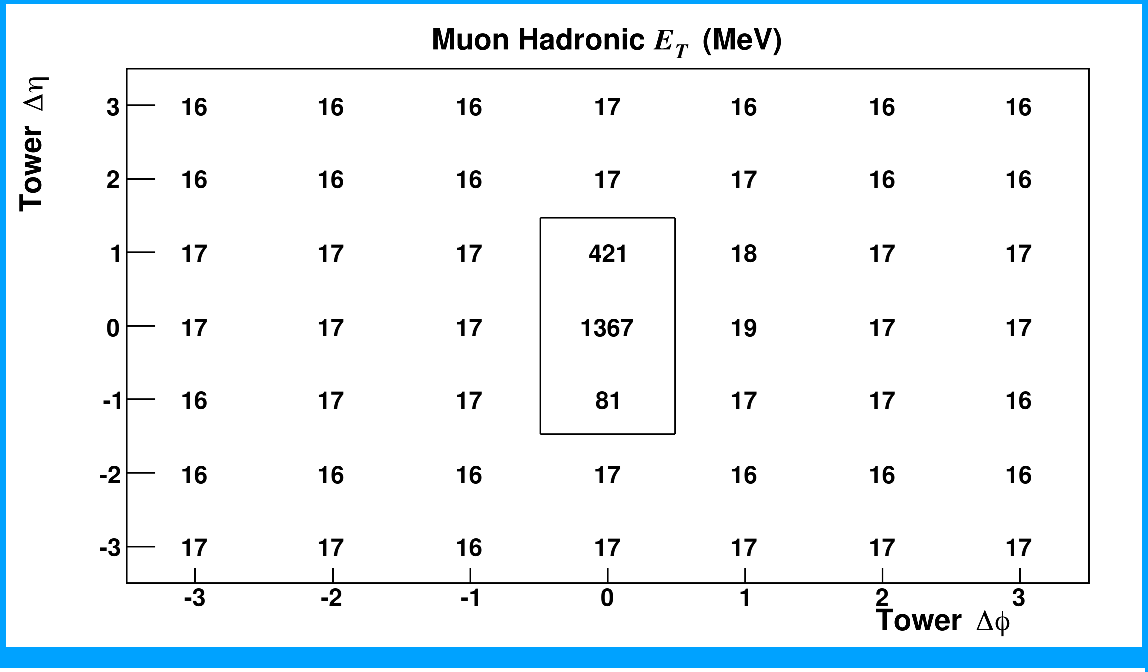

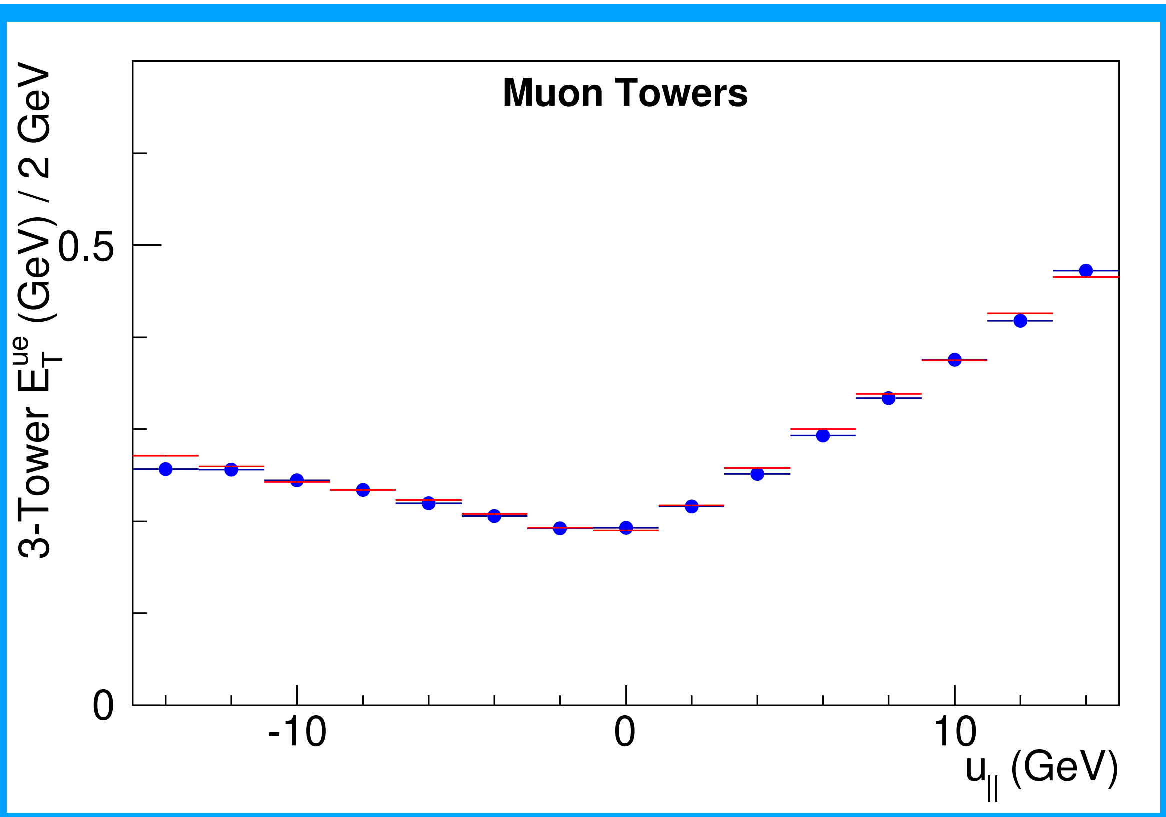

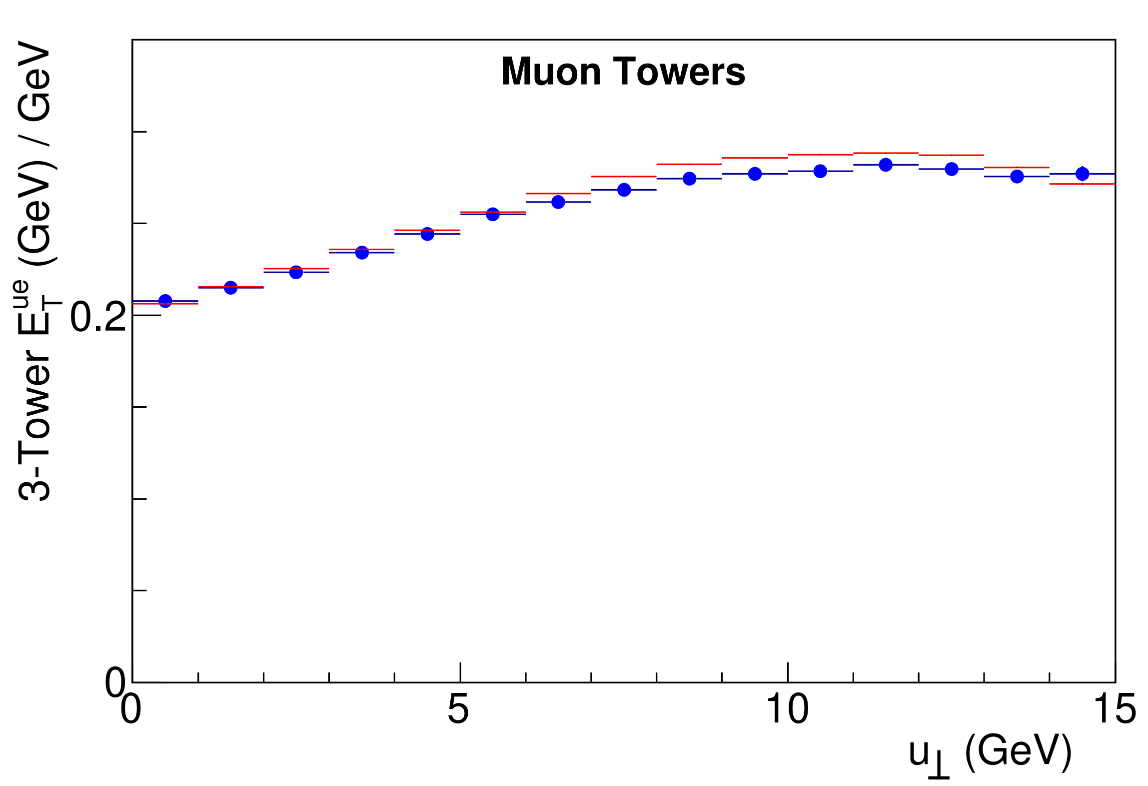

Electron momentum calibration

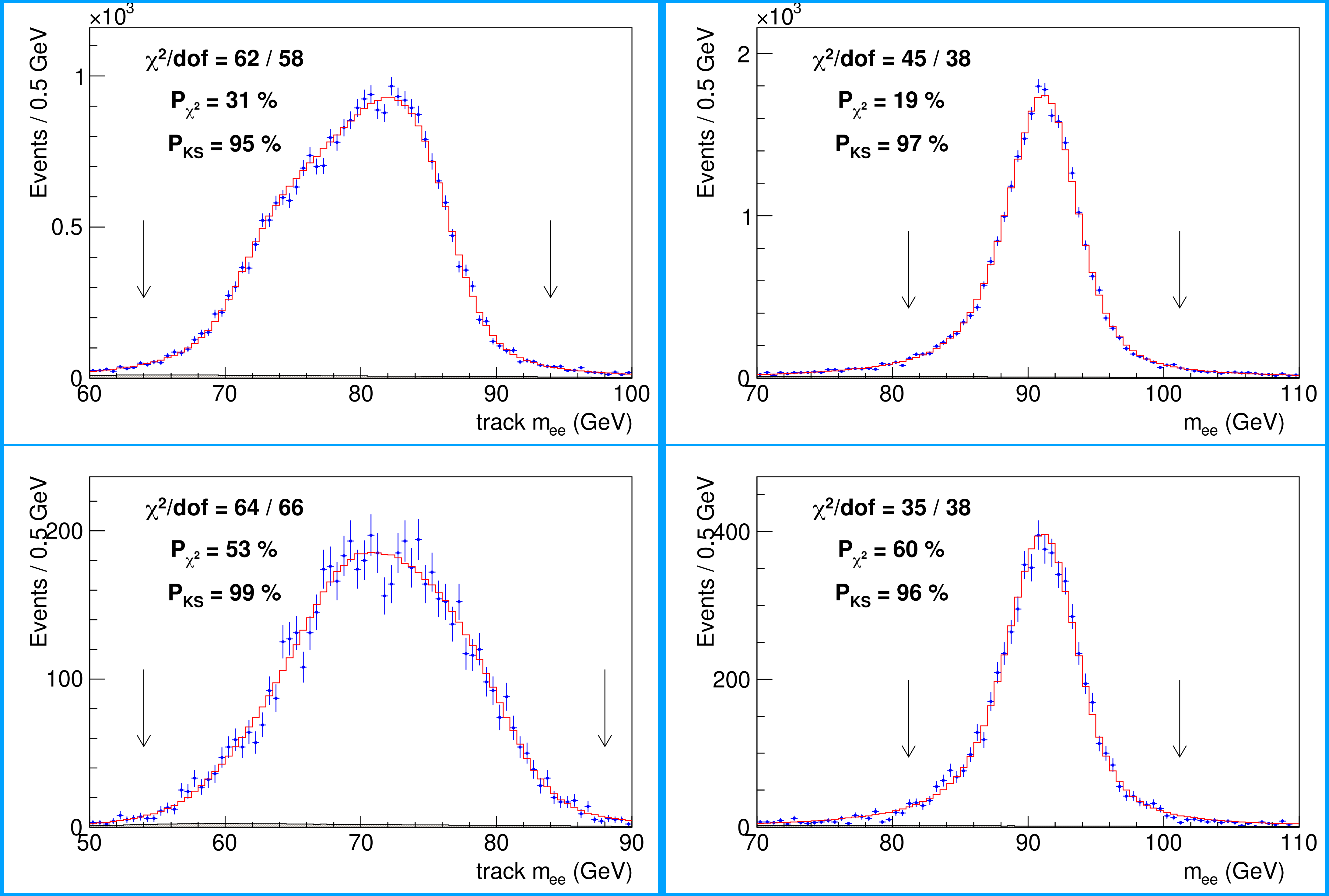

Z mass fits using tracker or calorimeter

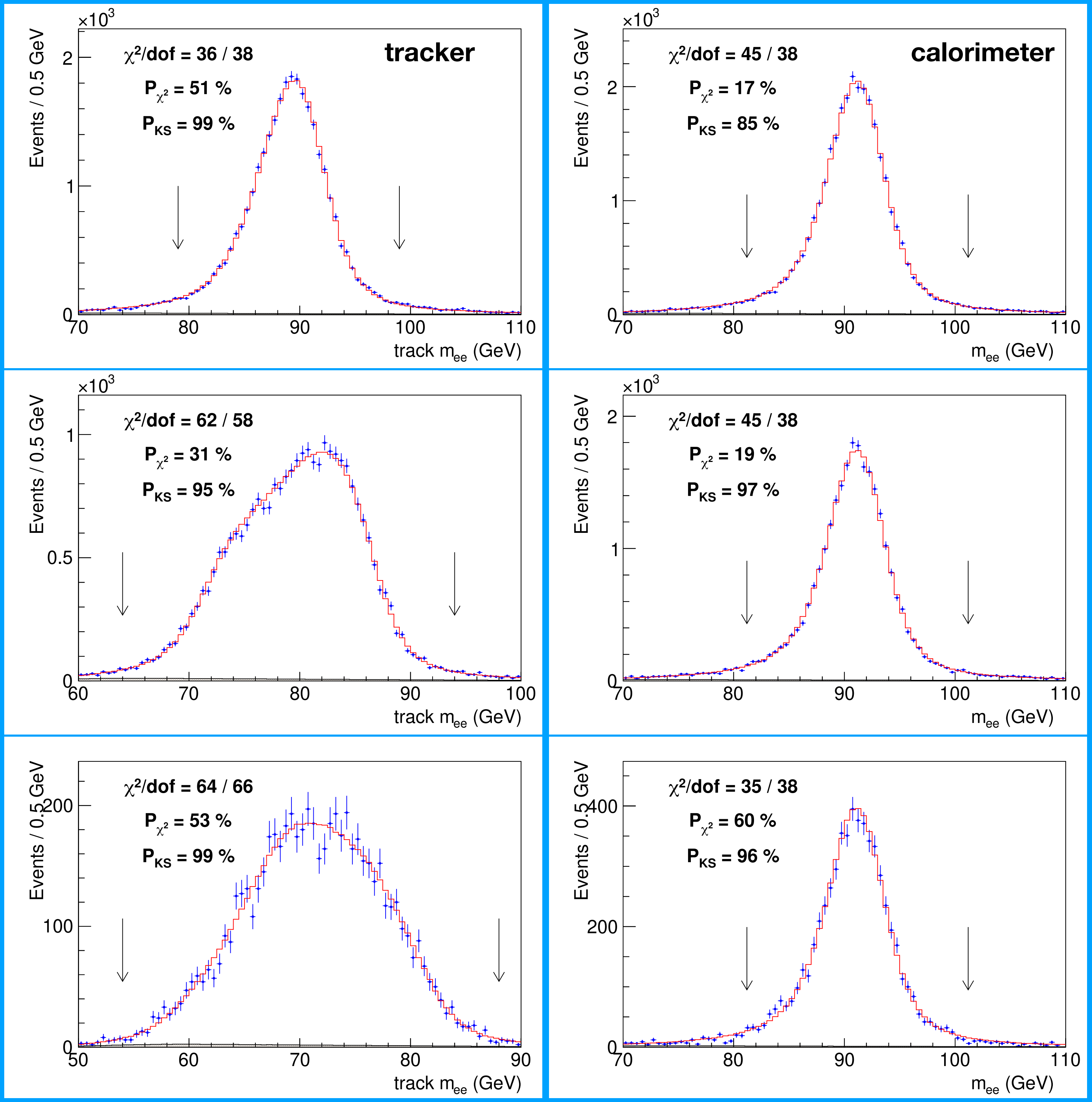

Electrons	Calorimeter	Track
$E/p < 1.1$ only	$91\,190.9 \pm 19.7$	$91\,215.2 \pm 22.4$
$E/p > 1.1$ and $E/p < 1.1$	$91\,201.1 \pm 21.5$	$91\,259.9 \pm 39.0$
$E/p > 1.1$ only	$91\,184.5 \pm 46.4$	$91\,167.7 \pm 109.9$

Muon momentum calibration

Third step is to calibrate the scale using Υ decays to muons

Compare fit results with and without constraining the track to the collision point

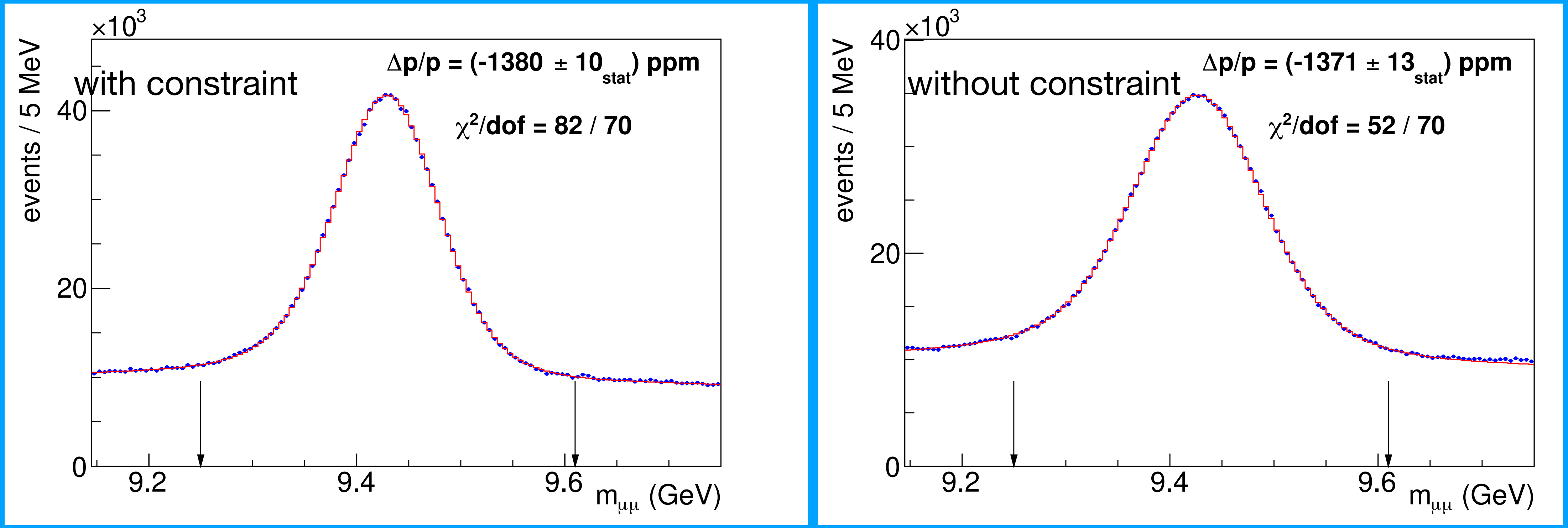

Source	J/ψ (ppm)	Υ (ppm)	Correlation (%)
QED	1	1	100
Magnetic field non-uniformity	13	13	100
Ionizing material correction	11	8	100
Resolution model	10	1	100
Background model	7	6	0
COT alignment correction	4	8	0
Trigger efficiency	18	9	100
Fit range	2	1	100
$\Delta p/p$ step size	2	2	0
World-average mass value	4	27	0
Total systematic	29	34	16 ppm
Statistical NBC (BC)	2	13(10)	0
Total	29	36	16 ppm

Muon momentum calibration

First step is to align the drift chamber (the “central outer tracker” or COT)

Two parameters for the electrostatic deflection of the wire within the chamber constrained using difference between fit parameters of incoming and outgoing cosmic-ray tracks

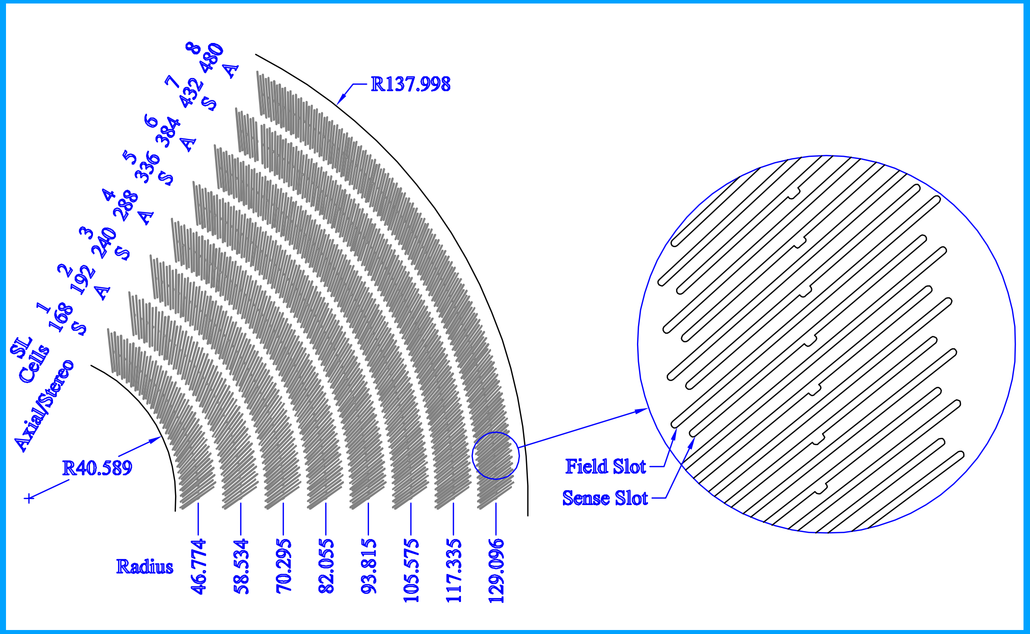

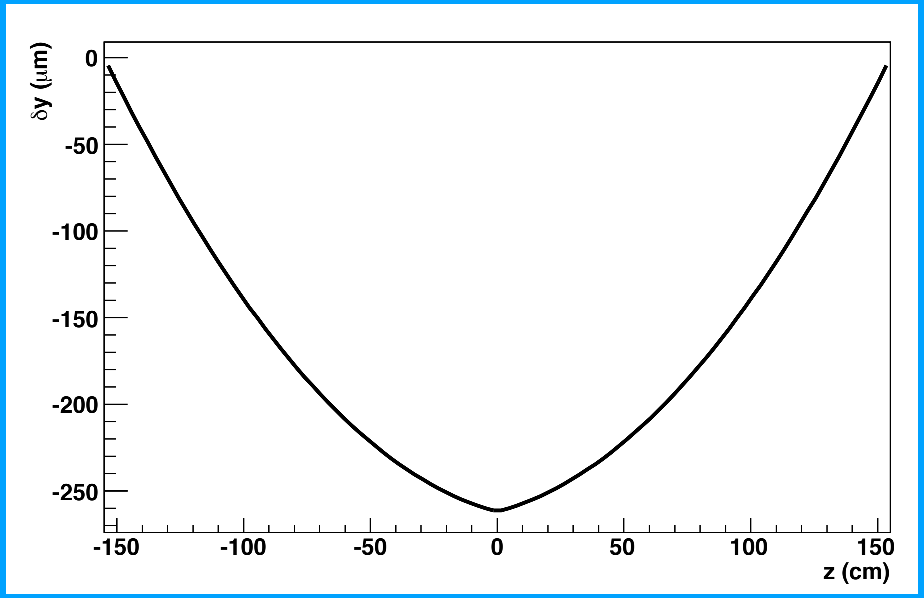

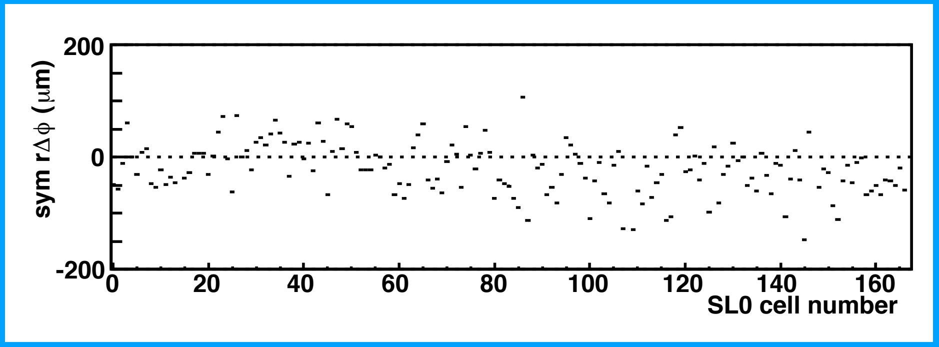

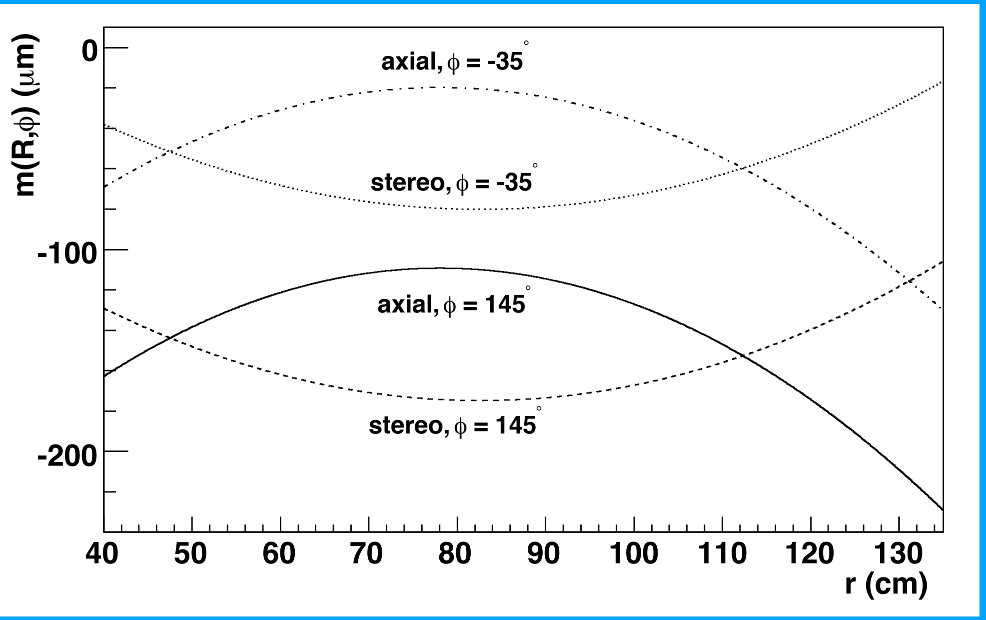

Track momentum calibration

Residual tracker misalignments studied using difference in E/p between electrons and positrons

Correction as a function of polar angle applied to measured tracks from W and Z decays

Linear dependence on cot theta would cause a bias in the m_W mass fit

No linear correction required, statistical precision from E/p constrains the bias to <0.8 MeV

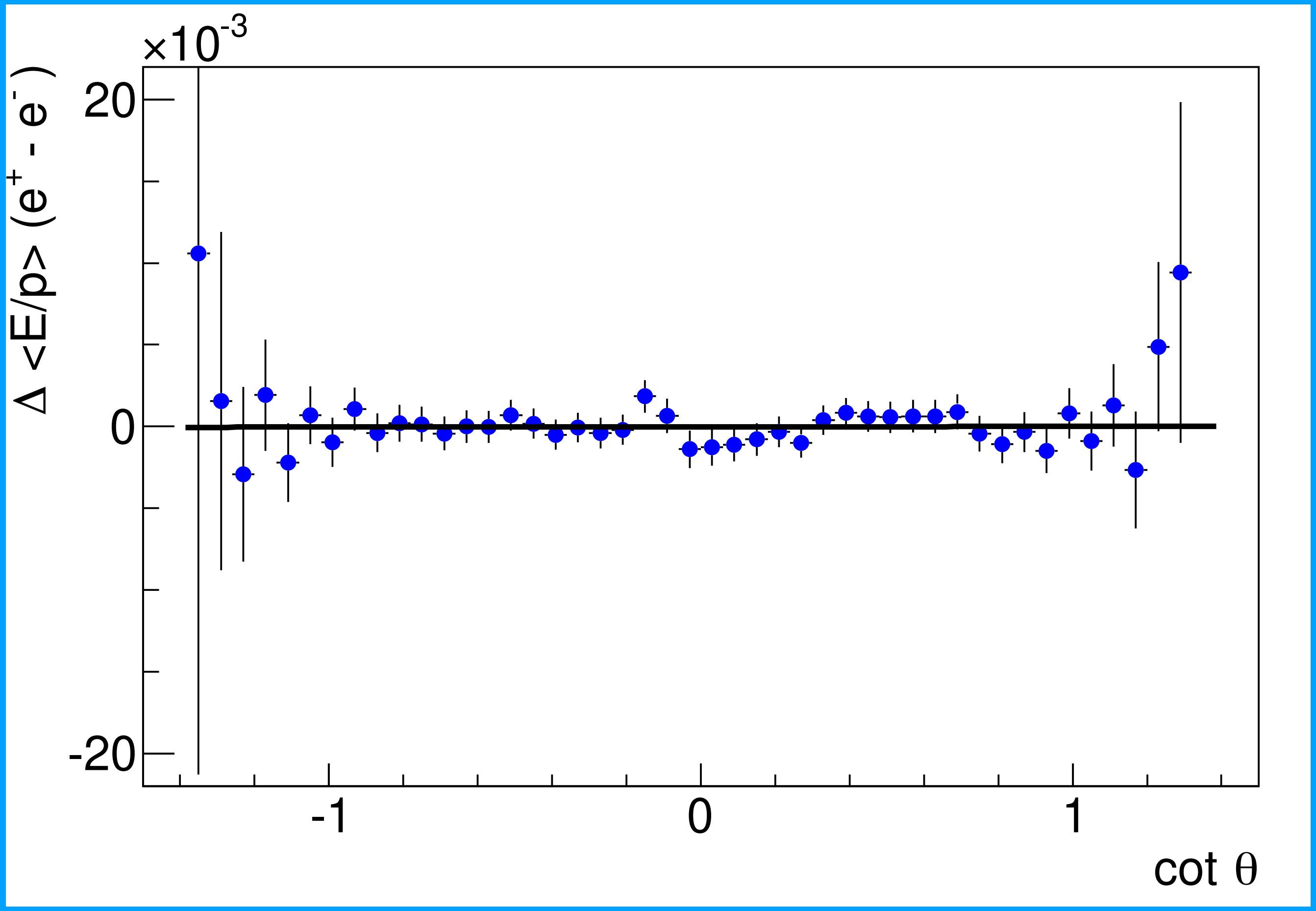

Detector simulation

Developed custom simulation for analysis
Models ionization energy loss, multiple scattering, bremsstrahlung, photon conversion, Compton scattering

Acceptance map for muon detectors

Parameterized GEANT4 model of electromagnetic calorimeter showers
Includes shower losses due to finite calorimeter thickness

Kotwal & CH, NIMA 729, 25 (2013)

Hit-level model of central outer tracker
Layer-by-layer resolution functions and efficiencies

Material map of inner silicon detector
Includes radiation lengths and Bethe-Bloch terms